Accepted Manuscript

Design, synthesis and biological evaluations of quaternization harman analogues as potential antibacterial agents

Jiangkun Dai, Wenjia Dan, Siyu Ren, Congguo Shang, Junru Wang

PII: S0223-5234(18)30874-2

DOI: 10.1016/j.ejmech.2018.10.012

Reference: EJMECH 10798

To appear in: *European Journal of Medicinal Chemistry*

Received Date: 26 January 2018

Revised Date: 16 September 2018

Accepted Date: 5 October 2018

Please cite this article as: J. Dai, W. Dan, S. Ren, C. Shang, J. Wang, Design, synthesis and biological evaluations of quaternization harman analogues as potential antibacterial agents, *European Journal of Medicinal Chemistry* (2018), doi: https://doi.org/10.1016/j.ejmech.2018.10.012.

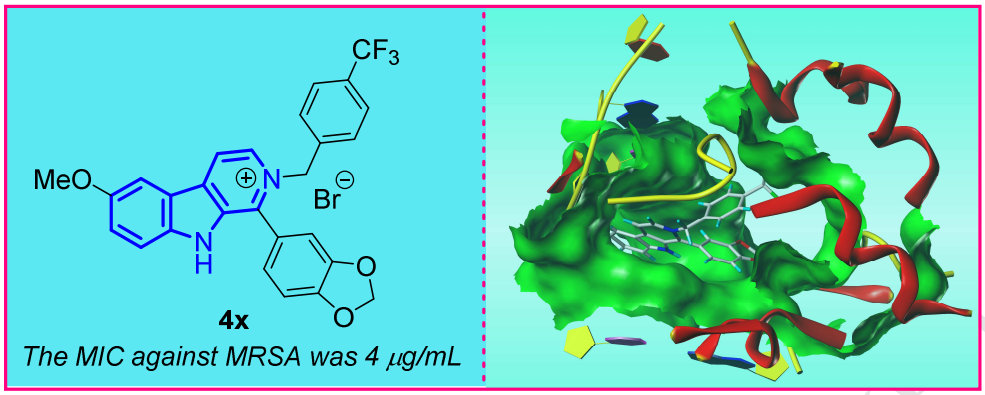

Design, synthesis and biological evaluations of quaternization harman analogues as potential antibacterial agents

Jiangkun Dai, Wenjia Dan, Siyu Ren, Congguo Shang, and Junru Wang*

College of Chemistry & Pharmacy, Northwest A&F University, 22 Xinong Road, Yangling 712100, Shaanxi, China.

***Corresponding author**

E-mail: wangjunru@nwafu.edu.cn (J.R. Wang)

ABSTRACT

Thirty-three new quaternization harman analogues were synthesized and their antibacterial activity against four Gram-positive and two Gram-negative bacteria were evaluated. The structure–activity relationships were summarized and compounds **4f**, **4i**, **4l**, **4u**, **4w**, **4x** and **5c** showed excellent antibacterial activity, low cytotoxicity, good thermal stability and "drug-like" properties. In particular, compound **4x** exhibited better bactericidal effect (4-fold superiority against methicillin-resistant *Staphylococcus aureus*) than standard drugs fosfomycin sodium and ampicillin sodium (minimum inhibitory concentration = 50 nmol/mL). Scanning electron microscopy revealed morphological changes of the bacterial cell surface and the docking evaluation provided a good total score (6.4952) for **4x** which is close to the score of ciprofloxacin (6.9723). The results indicated that the quaternization harman analogues might exert their bactericidal effect by damaging bacterial cell membrane and wall, and disrupting the function of type II topoisomerase. In addition, the *in vivo* antibacterial assay with a protective efficacy of 81.3% further demonstrated the potential of these derivatives as new bactericides and antibiotics.

Keywords: harman; quaternization; derivatization synthesis; bactericides; structure–activity relationships; molecular docking.

1. Introduction

Infections caused by bacterial pathogens are a major cause of morbidity and mortality worldwide. Although the successful treatment of such infections by antibiotic drugs is widely regarded as a major medical breakthrough of the 20th century, this achievement may not be sustainable in the future, as bacteria have counteracted antibiotic pressure and developed or acquired resistances that render formerly efficacious drugs inactive [1,2]. In recent years, the emergence of the antibiotic crisis has brought great challenges to normal production and life such as healthcare systems, farming, and the food production industry [3–5]. For example, the misuse and overuse of current antibiotics has resulted in a situation that higher dose is required to successfully treat the bacterial infection [6]. Moreover, the intensive antibacterial discovery effort has seen a dramatic decline in the large pharmacy industry in the last two decades [7]. "The cost in terms of lost global production between now and 2050 would be an enormous 100 trillion USD if we do not take action," as a UK Government report states [8]. Therefore, we need to develop new drugs to replace the ones that no longer work.

Natural products are an important source of antibacterial agents [9]. The seeds of *Peganum harmala*, containing about 2–6% pharmacologically active alkaloids which are mostly *β*-carbolines such as harman **L1** (Fig. 1), were used as antibacterial drugs many years ago in North Africa and Middle East [10]. Canthin-6-one **L4**, a subclass of *β*-carboline alkaloids with an additional D ring, isolated from *Allium neapolitanum*, showed good antibacterial activity (MIC = 8–64 μg/mL) against *S. aureus* [11]. Eudistomin U **L6**, *β*-carboline with an additional indole ring at position 1, isolated from several species of marine ascidians, also exhibited good antibacterial activity (IC_{50} = 6.4 μg/mL) [12]. In our previous work, we also reported the antibacterial activity of some modified *β*-carbolines **L2**–**L5** [13,14].

With the aim of finding more promising antibacterial harman analogues, we report here a strategy to generate the bioactive compounds. Our idea and design are relatively simple (Fig. 1). Briefly, considering the antibacterial activity data of **L2** and

L3, we speculate that the substituents at position 1 are favorable. Simultaneously, the activity data of **L1** and **L6** indicate that the aromatic substituents are more potent. So we deduce that an additional aromatic substituent at position 1 might improve the bactericidal effect of harman. Our previous work showed that some N^3-substituted canthin-6-ones **L5** exhibited approximate 32-fold advantage against *S. aureus* (MIC = 0.98 μg/mL) over canthin-6-one **L4** (MIC = 31.25 μg/mL) [13]. The result indicates that quaternization derivatives might be promising. During the course of our initial efforts to improve the antibacterial activity of harman **L1**, we confirmed the main skeleton of the leading compound **L7** based on the vital factors mentioned. In order to enrich the chemical diversity as well as to further study the structure–activity relationships, the quaternization harman analogues incorporating the methoxy group at position 6 were also synthesized. The synthesized compounds were characterized and tested for their *in vitro* and *in vivo* antibacterial activity. In addition, their structure–activity relationships, cytotoxicity, thermal stability, "drug-like" properties and preliminary antibacterial mechanism were studied.

2. Results and Discussion

2.1. Chemistry

The initial synthetic aim was to obtain a convenient route for the preparation of quaternization harman analogues. So, it was decided to begin with the preparation of **2a**–**2h** (yield: 92%–96%) through the Pictet–Spengler reaction [15]. Compounds **3a**–**3h** (yield: 62%–73%) were then easily obtained using a palladium catalyst [16]. Subsequently, the quaternization reaction was carried out at room temperature [17]. The synthesis of the target compounds **4a**–**4x** (yield: 67%–96%) is shown in Fig. 2. In order to clarify the influence of different substituted benzyl groups on activity, compounds **5a**–**5i** (yield: 72%–95%) were synthesized as shown in Fig. 3. Nuclear magnetic resonance (NMR) spectroscopy (^{1}H NMR, ^{13}C NMR, DEPT 135, heteronuclear multiple-bond correlation, heteronuclear single quantum correlation, and homonuclear correlation spectroscopy) of **4q** confirmed that the benzylation position is N^2 (Fig. S1). The successful synthesis of the intermediates **3a**–**3h** and the

quaternization harman derivatives (**4a**–**4x** and **5a**–**5i**) was further confirmed by crystal structures of the compounds **3e** and **5f** (Fig. 4). Moreover, these two crystal structures further guided the structural confirmation of all the 41 compounds. The x-ray data block (bond lengths, bond angles *etc.*) of compounds **3e** and **5f** has been presented in Supplementary data.

All spectral and analytical data were consistent with the assigned structures. In the NMR spectra of compound **3a**, the signals of the methyl group were detected around δ = 3.94 ppm (^{1}H NMR) and δ = 52.2 ppm (^{13}C NMR). The signal of the imino hydrogen atom was observed at δ = 8.81 ppm (^{1}H NMR) and the signals of the phenyl hydrogen atoms appeared in the aromatic region. Moreover, the signal of the carbonyl carbon atom was detected around δ = 166.8 ppm (^{13}C NMR). After quaternization, the signals of the methylene group were detected around δ = 5.82 ppm (^{1}H NMR) and δ = 60.9 ppm (^{13}C NMR) in the NMR spectra of compound **4a**, which indicated that the quaternization harman derivatives were successfully synthesized. In addition, the signals of the carbonyl could be found at 1718 and 1712 cm^{-1} in the IR spectra of compounds **3a** and **4a**, respectively.

2.2. Antibacterial activity

Bacteria could be divided into two categories by Gram staining, Gram-positive and Gram-negative bacteria. *S. aureus* and MRSA are the leading causes of bacterial infections in humans with symptoms ranging from simple skin infections to severe necrotizing fasciitis and pneumonia [18]. *Bacillus cereus* and *Escherichia coli* could cause food poisoning, such as a diarrheal syndrome and an emetic syndrome, both through the production of distinct toxins [19]. *Bacillus subtilis* and *Ralstonia solanacearum* are major components of plant pathogens [20]. So four Gram-positive bacteria (*S. aureus* CGMCC 1.8721, MRSA ATCC 43300, *B. cereus* CGMCC 1.1846, and *B. subtilis* 769) and two Gram-negative bacteria (*E. coli* CGMCC 1.1636 and *R. solanacearum* CGMCC 1.12711) were selected as the tested bacteria in this work. Compounds (**3a**–**3h**, **4a**–**4x** and **5a**–**5i**) were evaluated for their *in vitro* antibacterial activity through double dilution method, with fosfomycin sodium, ampicillin sodium,

and cefotaxime sodium as the positive controls.

The antibacterial results (Table 1) revealed that most of the quaternization harman analogues displayed good *in vitro* biological activity against all of the tested bacterial strains except for *E. coli*. Although most of the intermediates were inactive under the tested concentrations, compound **3h** exhibited weak activity (MIC = 200 nmol/mL) against MRSA and *S. aureus*. Compared with the positive control fosfomycin sodium, compounds **4a**–**4l**, **4n**–**4o** and **4q**–**4x** were found to be the most potent compounds against *S. aureus*, with peak MICs of lower than 25 nmol/mL. Six compounds (**4f**, **4i**, **4l**, **4u**, **4w** and **4x**) displayed equal or superior activity against MRSA compared with the positive controls. Fifteen compounds exhibited better activity against *B. cereus* than ampicillin sodium. Specifically, the MIC of **4f** and **4x** (25 nmol/mL) was equal to that of the positive controls fosfomycin sodium and cefotaxime sodium. Nine compounds (**4f**, **4h**, **4i**, **4k**, **4l**, **4t**, **4u**, **4w** and **4x**) showed a potential MIC (25 nmol/mL) against *B. subtilis*. As shown in Table 1, eight compounds (**4f**, **4h**, **4i**, **4k**, **4l**, **4u**, **4w** and **4x**) exhibited better activity (MIC = 25 nmol/mL) against *R. solanacearum* than fosfomycin sodium (MIC = 50 nmol/mL). The activity of different substituted benzyl derivatives was tested (Table 2), and compound **5c** was considered to be the compound with the most potential. Interestingly, other quaternization harman analogues also showed similar effects on different bacteria. For example, the MIC of the compound 2,6-dimethyl-9*H*-pyrido[3,4-*b*]indol-2-ium iodide against MRSA was 4 μg/mL [21].

2.3. Structure–activity relationships

Based on the antibacterial activity data, the structure–activity relationships were carefully investigated (Fig. 5). The derivatives containing a methoxy group at position 6 were practically the same or higher than that derivatives without this group, with the exception of pyridine. For example, the MIC of compound **4f** was 25 nmol/mL against *S. aureus*, which was better than **4c** (MIC = 50 nmol/mL). Compared with harman **L1** (MIC = 1000 μg/mL, ≈ 5494 nmol/mL), compound **3h** displayed better activity (MIC = 200 nmol/mL) against *S. aureus*, which indicates that an aromatic

group at position 1 is effective. Comprehensive analysis indicated that the benzo[*d*][1,3]dioxole group is the most effective substituent at position 1, and the furan group is better than the methyl benzoate group. For example, the MIC against MRSA of compound **4x** was 12.5 nmol/mL, which was better than compounds **4f** (25 nmol/mL), **4l** (25 nmol/mL) and **4r** (100 nmol/mL). Compared with compound **4c** (MIC = 50 nmol/mL against *R. solanacearum*), with a methyl benzoate group substituent at position 1, the MIC of compound **4i** (furan group at position 1, MIC = 25 nmol/mL against *R. solanacearum*) is better.

Quaternization is clearly beneficial for improving antibacterial potency. Various substituted benzyl groups have a significant effect on the activity. The influence of different groups is easily seen in Table 1 and Table 2: CF_3 > Br > Cl ≈ CH_3 > F ≈ NO_2. For example, the MIC of compound **4f** was 25 nmol/mL against all the tested bacteria except for *E. coli*. In addition, the MICs of compounds **5c (**25 nmol/mL against *S. aureus*), **5f (**75 nmol/mL against *S. aureus*) and **5g (**50 nmol/mL against *S. aureus*) indicate the activity sequence for substituents at different positions: *para* > *meta* > *ortho*. Interestingly, similar findings have been reported by others, which supported our SAR results (*para* substituents are better) and confirmed the advantages of trifluoromethyl group [22].

2.4. Cell toxicity and molecular physicochemical properties

Many natural and synthetic agents with the ability to interact with DNA often have relatively low therapeutic index, most likely due to the unspecific manner of these agents in causing DNA damage both in lesions and in highly proliferative normal tissues. Similarly, the frequency of utilization of *β*-carbolines as therapeutic agents is greatly reduced because of their cytotoxic activity toward mammalian cells (low selectivity) [23]. We determined the cytotoxic effects of the highly bioactive quaternization harman derivatives **4f**, **4i**, **4l**, **4u**, **4w**, **4x** and **5c** on MARC 145 cells (normal monkey kidney cells) and L02 cells (normal human hepatocyte) [24]. Simultaneously, the activity under mass concentration was also tested. As shown in Table 3, the cell viabilities of all the tested compounds were more than 87% on

MARC 145 cells and more than 71% on human hepatocyte L02 cells. The results suggest that these molecules are of low toxicity. Interestingly, compound **4x** exhibited excellent viability (103%) on MARC 145 cells under an effective antibacterial dose (8 μg/mL).

In 1997, Lipinski *et al.* published what is widely regarded as the key paper defining physicochemical and structural properties profiles for the optimal oral availability of drugs [25]. In 2003, Clarke and Delaney reported that most herbicides and fungicides also adhere to the Lipinski rule [26]. As we know, for good oral bioavailability an ideal molecule should have good intestinal absorption and reduced molecular flexibility [27]. The molecular properties of the preferred ionic derivatives are shown in Table 4. For all the preferred compounds, the log *P* values were lower than 5, the number of hydrogen bond acceptors were lower than 10, the number of rotatable bonds were lower than 10, and the number of hydrogen bond donors were lower than 5. Their physicochemical data therefore conform to the Lipinski rule without considering the molecular weight, which demonstrate they might have good "drug-like" properties. Further, the topological polar surface area (TPSA), a parameter defined as the surface sum over all polar atoms and used extensively in medicinal chemistry to predict absorption and optimize a compound's membrane permeability, was calculated for the potent compounds. It is suggested that compounds with a TPSA greater than 140 $Å^2$ tend to be poor at permeating cell membranes [27]. Based on the predicted data mentioned above, the calculated TPSA values for the highly bioactive quaternization harman derivatives would indicate a possible good bioavailability.

*2.5. Thermal stability of compound **4x** in vitro* [28,29]

Considering the poor thermal stability of antibiotics, it was decided to further investigate the bioactive compound **4x** using an *in vitro* assay, to consider whether its thermal stability had improved compared with the control. As depicted in Fig. S2, ampicillin sodium began to degrade after being kept at 37 °C for 6 h. After being kept at 65 °C for 6 h, very little ampicillin sodium residue could be found. Compound **4x**

did not degrade any further under the same conditions.

2.6. Scanning electron microscopy analysis

SEM of MRSA and *R. solanacearum* revealed morphological changes in the bacterial cell surface (Fig. 6). The surfaces of cells in the untreated group (Fig. 6A and 6C) were relatively smooth and regular, whereas when treated with compound **4x** (Fig. 6B and 6D) there was shrinkage. Increased permeabilization of the membrane may explain the leakage of cytoplasmic material. Additionally, bacteria exposed to the compound **4x** experienced cell wall disintegration. These results indicated that compound **4x** may exert its bactericidal effect by damaging bacterial cell membrane and wall.

2.7. Molecular docking study

The Surflex-Dock scoring function is a weighted sum of non-linear functions based on the binding affinities of protein-ligand complexes coupled with their crystallographically determined structures. Surflex-Dock scores are expressed in $-\log_{10}(K_d)$ units to represent binding affinities [30,31]. Type II topoisomerase present in bacteria is attractive target for antibacterial drug discovery, which is independently essential for bacterial DNA replication [32]. Mechanism of topoisomerases inhibition is known to occur in two ways: these inhibitors may bind with topoisomerase directly or they may bind to DNA and alter its structure, so that it cannot be recognized by topoisomerases [33]. A previous study demonstrated that large planar surface areas could function at the DNA level via intercalation between base pairs. Further, it was shown that DNA intercalation of molecules could disrupt the function of topoisomerases, ultimately leading to cell death [18]. For quaternization harman analogues, *β*-carboline core *per se* is a planar molecule. In some extent, their structures are also similar to the commercial antibiotic ciprofloxacin which targets to the type II topoisomerase. So we selected a crystal of bacterial type II topoisomerase complex (PDB ID: 5IWM) as a possible target.

A docking investigation based on the Surflex-Dock program in the Sybyl-X 2.0

package was undertaken to explore the possible mechanism. Firstly, we performed a re-docking of the extracted co-crystallized ligand present in the type II topoisomerase complex. The RMSD (root-mean-square deviation) value was 0.923Å (< 2.0 Å), which indicated the docking protocol was feasible [34, 35]. The highly active compound **4x** gave a good total score (6.4952) which was close to the score of the standard compound ciprofloxacin (6.9723). Interestingly, the MIC value of ciprofloxacin against *S. aureus* (4 μg/mL) further supported the rationality of the docking protocol. As shown in Fig. 7, compound **4x** mainly bound to DNA area. There are many π–π stacked interactions between the plane structure of the small molecule and the DNA base (DA10, DA11, DT10, and DT11). The hydrogen atom of the methoxy group is adjacent to the DNA base (DC12), forming two carbon–hydrogen bonds (2.65 and 2.69 Å). The trifluoromethyl fragment of compound **4x** is adjacent to the ASP83 residue of the target, forming a strong halogen bond with a length of 2.73 Å. Simultaneously, two carbon–hydrogen bonds (2.32 and 2.50 Å) are formed between the trifluoromethyl group and the SER84 residue. Interestingly, the interaction of the trifluoromethyl group confirms the activity and structure–activity relationship finding that trifluoromethyl fragments are beneficial for improving antibacterial activity.

As we all known, there are two types of topoisomerase, namely, type I topoisomerase and type II topoisomerase [36]. In order to check the selectivity of the titled compounds against type II topoisomerase over type I topoisomerase, a docking investigation between compound **4x** and type I topoisomerase complex (PDB ID: 4RUL) was also undertaken. The total score was 4.0326 which indicated that compound **4x** showed approximately 290-fold selectivity against type II topoisomerase over type I topoisomerase (Total score = $-\log_{10}(K_d)$, $K_a \times K_d = 1$, K_d represent dissociation constant, K_a represent binding constant, selectivity = K_a(type II topoisomerase) / K_a(type I topoisomerase)).

Considering with the SEM results, we deduced that compound **4x** might attack and cause damage to the bacterial cell membrane and wall. The consequent increased permeability of the bacterial cell membrane will then allow compound **4x** to enter the

cells. The **4x** in the cytoplasm will then disrupt the function of type II topoisomerase, which in turn caused cell death.

2.8. Protective effect in vivo[37,38]

The *in vivo* antibacterial activity (protective effect) of the highly bioactive compound **4x** was tested against *R. solanacearum* on eggplant leaf (Fig. 8). Compound **4x** was found to have a good preventative effect against *R. solanacearum*, with a protective efficacy of 81.3%. This demonstrates the potential of the quaternization harman derivatives as new bactericides.

3. Conclusions

In summary, 41 compounds, including 33 new quaternization harman derivatives, were prepared via a convenient synthetic route and their antibacterial activity was evaluated. The structure–activity relationships were summarized which provided some important guidance for the development of antibacterial harman agents. The highly bioactive compounds **4f**, **4i**, **4l**, **4u**, **4w**, **4x** and **5c**, with a peak MIC of 4 μg/mL, showed low cytotoxicity, good thermal stability and “drug-like” properties. Further, the SEM analysis and molecular docking evaluations suggested multiple possible antibacterial targets of quaternization harman analogues, namely membrane, wall and type II topoisomerase. As expected, the *in vivo* antibacterial assay demonstrated the potential of the quaternization harman agents as new bactericides and antibiotics. Overall, this work enriched the types of candidate antibiotics and provided more options for solving the current antibiotic crisis.

Chirality of drugs is an eternal topic in medicinal chemistry. For some highly active quaternization harman molecules, chiral axis is existed at position 1. In order to separate the isomers, we have used twelve different separation conditions (Supplementary data). Regrettably, we did not get the isomers. Here, we are to appeal to researchers to further study this issue to promote the development and application of quaternization harman antibiotics.

4. Experimental

4.1. Materials

^{1}H NMR and ^{13}C NMR spectroscopy was carried out using an Avance spectrometer (Bruker, Billerica, MA, USA) at 500 and 125 MHz. Chemical shifts were measured relative to the residual solvent peaks of CD_3OD (^{1}H, δ = 3.31 ppm; ^{13}C, δ = 49.00 ppm) or dimethyl sulfoxide (DMSO-d_6) (^{1}H, δ = 2.50 ppm; ^{13}C, δ = 39.52 ppm) with tetramethylsilane as the internal standard. High-resolution mass spectroscopy (HRMS) was undertaken using an AB SCIEX Triple TOF 5600^{+} spectrometer. Liquid chromatography–electrospray ionization–tandem mass spectrometry (LC-ESI-MS/MS) analysis was accomplished using ultra-high-performance liquid chromatography (UHPLC) (Nexera UHPLC LC-30A) coupled to an AB SCIEX Triple TOF 5600^{+} spectrometer, with the system equipped with a C18 trap column (Shim-pack XR-ODS, 2.0 mm i.d. × 100 mm). Elemental analyses were performed on a Heraeus CHN-O-Rapid instrument. Compounds **3e** and **5f** were collected at 100 K on a Rigaku Oxford Diffraction Supernova Dual Source, Cu at Zero equipped with an AtlasS2 CCD using Cu Kα radiation. Data reduction was carried out with the diffractometer's software Scanning electron microscopy (SEM) analysis was carried out on Nova nano SEM450 instrument. Molecular docking evaluation was conducted with the Sybyl-X 2.0 software and Discovery Studio 2017 client. Fourier transform infrared (FT-IR) spectra were obtained on a TENSOR37 spectrometer (Bruker) using KBr pellets, and the absorptions are reported in cm^{-1}. The reaction progress was monitored by thin-layer chromatography (TLC) on silica gel GF254 (Qingdao Haiyang Chemical Co., Ltd., Qingdao, China) with ultraviolet detection. Reagents were purchased from commercial sources (Bodi Chemical Co., Ltd., Tianjin, China; Aladdin Industrial Co., Ltd., Shanghai, China), and used as received.

4.2. Synthesis

*4.2.1. Synthesis of intermediates **3a–3h***

A solution of tryptamine (1.6 g, 10 mmol) or 5-methoxytryptamine (1.9 g, 10

mmol), aldehyde (methyl 4-formylbenzoate, furfural, pyridine-2-carboxaldehyde, or piperonyl aldehyde) (11 mmol), and trifluoroacetic acid (100 μL) in dichloromethane (50 mL) was stirred at room temperature for 36 h. Dichloromethane (30 mL) and ammonia water (5%, 30 mL) were added, and the organic layer was separated. Next, the water phase was extracted with dichloromethane, and the organic phases were combined and dried over sodium sulfate and filtered. The solvent was then evaporated, and the crude product purified by column chromatography (ethyl acetate as the eluent) to give the products **2a**–**2h** in 92–96% yield. Pd/C (10%, 0.1 eq) was then added to the solution of **2a**–**2h** in xylene (50 mL), and the solution was heated at 145 °C and monitored by TLC. On completion, the resulting mixture was filtered and evaporated. The residue was purified by silica gel column chromatography with petroleum ether and ethyl acetate (v/v = 2:1) to produce **3a**–**3h** in 62–73% yield.

*4.2.1.1. methyl 4-(9H-pyrido[3,4-b]indol-1-yl)benzoate (**3a**)*: white solid; yield, 65%; m.p. 147.4–148.3 ^{o}C; ^{1}H NMR (500 MHz, $CDCl_3$) δ 8.81 (s, 1H), 8.58 (d, J = 2.5 Hz, 1H), 8.19–8.17 (m, 3H), 8.02 (d, J = 5 Hz, 2H), 7.97 (d, J = 5 Hz, 1H), 7.59–7.53 (m, 2H), 7.33 (t, J = 7.5 Hz, 1H), 3.94 (s, 3H); ^{13}C NMR (125 MHz, $CDCl_3$) δ 166.8, 142.9, 142.8, 141.5, 140.5, 139.6, 133.6, 130.4, 130.2, 128.8, 128.1, 121.9, 121.8, 120.5, 114.4, 111.6, 52.2. IR (KBr, cm^{-1}) 3362, 3065, 2957, 1718, 1637, 1619, 1582, 1526, 1497, 1469, 1438, 1326, 1294, 1279, 1223, 1164, 1128, 1067, 1026, 1015, 825, 792, 769, 726. Elemental anal. calcd for $C_{19}H_{14}N_2O_2$: C, 75.48; H, 4.67; N, 9.27; found C, 75.44; H, 4.69; N, 9.31. HRMS (ESI) m/z calcd for $C_{19}H_{14}N_2O_2$ $[M+H]^+$ 303.1128, found 303.1127.

*4.2.1.2. methyl 4-(6-methoxy-9H-pyrido[3,4-b]indol-1-yl)benzoate (**3b**)*: yellow solid; yield, 62%; m.p. 124.1–125.3 ^{o}C; ^{1}H NMR (500 MHz, $CDCl_3$) δ 8.84 (s, 1H), 8.57 (d, J = 5 Hz, 1H), 8.19 (d, J = 10 Hz, 2H), 8.05 (d, J = 10 Hz, 2H), 7.96 (d, J = 2.5 Hz, 1H), 7.63 (s, 1H), 7.48 (d, J = 10 Hz, 1H), 7.26 (d, J = 10 Hz, 1H), 3.99 (s, 3H), 3.97 (s, 3H); ^{13}C NMR (125 MHz, $CDCl_3$) δ 166.8, 154.5, 142.9, 141.7, 139.1, 135.5, 134.3, 130.3, 130.2, 130.1, 128.1, 122.1, 118.8, 114.3, 112.5, 103.6, 56.0, 52.2. IR (KBr, cm^{-1}) 3064, 2998, 2951, 2832, 1722, 1609, 1584, 1495, 1468, 1436, 1400, 1286,

1218, 1177, 1132, 1116, 1037, 1014, 818, 768. Elemental anal. calcd for $C_{20}H_{16}N_2O_3$: C, 72.28; H, 4.85; N, 8.43; found C, 72.26; H, 4.83; N, 8.47. HRMS (ESI) m/z calcd for $C_{20}H_{16}N_2O_3$ $[M+H]^+$ 333.1234, found 333.1230.

*4.2.1.3. 1-(furan-2-yl)-9H-pyrido[3,4-b]indole (**3c**)*: brown solid; yield, 66%; m.p. 127.1–128.6 ^oC; ^1H NMR (500 MHz, $CDCl_3$) δ 9.54 (s, 1H), 8.50 (d, J = 2.5 Hz, 1H), 8.15 (d, J = 5 Hz, 1H), 7.89 (d, J = 2.5 Hz, 1H), 7.71 (s, 1H), 7.60 (s, 2H), 7.35 (s, 2H), 6.67 (s, 1H); ^{13}C NMR (125 MHz, $CDCl_3$) δ 154.4, 142.8, 140.5, 138.8, 133.4, 131.3, 130.3, 128.6, 121.7, 121.2, 120.1, 113.7, 112.3, 111.6, 108.8. IR (KBr, cm^{-1}) 3458, 1625, 1556, 1493, 1452, 1425, 1378, 1366, 1318, 1301, 1284, 1252, 1235, 1210, 1164, 998, 749, 458. Elemental anal. calcd for $C_{15}H_{10}N_2O$: C, 76.91; H, 4.30; N, 11.96; found C, 76.87; H, 4.35; N, 11.94. HRMS (ESI) m/z calcd for $C_{15}H_{10}N_2O$ $[M+H]^+$ 235.0866, found 235.0863.

*4.2.1.4. 1-(furan-2-yl)-6-methoxy-9H-pyrido[3,4-b]indole (**3d**)*: brown solid; yield, 68%; m.p. 66.4–67.8 ^oC; ^1H NMR (500 MHz, $CDCl_3$) δ 9.30 (s, 1H), 8.41 (d, J = 5 Hz, 1H), 7.80 (d, J = 5 Hz, 1H), 7.67 (d, J = 2.5 Hz, 1H), 7.53 (d, J = 5 Hz, 1H), 7.46 (d, J = 10 Hz, 1H), 7.29 (d, J = 2.5 Hz, 1H), 7.22–7.20 (m, 1H), 6.64–6.63 (m, 1H), 3.93 (s, 3H); ^{13}C NMR (125 MHz, $CDCl_3$) δ 154.5, 154.2, 142.7, 138.3, 135.3, 133.6, 131.9, 130.0, 121.6, 118.6, 113.5, 112.4, 112.3, 108.7, 103.4, 56.0. IR (KBr, cm^{-1}) 2923, 1606, 1585, 1556, 1489, 1462, 1437, 1379, 1287, 1253, 1215, 1163, 1125, 1020, 810, 772, 738, 622. Elemental anal. calcd for $C_{16}H_{12}N_2O_2$: C, 72.72; H, 4.58; N, 10.60; found C, 72.68; H, 4.60; N, 10.58. HRMS (ESI) m/z calcd for $C_{16}H_{12}N_2O_2$ $[M+H]^+$ 265.0972, found 265.0970.

*4.2.1.5. 1-(pyridin-2-yl)-9H-pyrido[3,4-b]indole (**3e**)*: white solid; yield, 70%; m.p. 139.4–141.2 ^oC; ^1H NMR (500 MHz, $CDCl_3$) δ 11.27 (s, 1H), 8.71–8.69 (m, 2H), 8.50 (d, J = 5 Hz, 1H), 8.09 (d, J = 5 Hz, 1H), 7.93 (d, J = 5 Hz, 1H), 7.83–7.80 (m, 1H), 7.56–7.50 (m, 2H), 7.24–7.22 (m, 2H); ^{13}C NMR (125 MHz, $CDCl_3$) δ 158.0, 148.2, 140.6, 138.1, 138.1, 136.8, 134.8, 130.5, 128.4, 122.9, 121.7, 121.3, 121.1, 119.8, 115.4, 111.9. IR (KBr, cm^{-1}) 3395, 3291, 3057, 1625, 1588, 1564, 1484, 1446, 1414, 1362, 1316, 1280, 1234, 1146, 1091, 1065, 798, 743, 622, 597. Elemental anal.

372 calcd for $C_{16}H_{11}N_3$: C, 78.35; H, 4.52; N, 17.13; found C, 78.33; H, 4.55; N, 17.10.
373 HRMS (ESI) m/z calcd for $C_{16}H_{11}N_3$ $[M+H]^+$ 246.1026, found 246.1025.

374 *4.2.1.6. 6-methoxy-1-(pyridin-2-yl)-9H-pyrido[3,4-b]indole (**3f**)*: white solid; yield,
375 73%; m.p. 131.4–132.2 ^oC; ^1H NMR (500 MHz, $CDCl_3$) δ 11.09 (s, 1H), 8.67 (d, J =
376 10 Hz, 1H), 8.64 (d, J = 5 Hz, 1H), 8.44 (d, J = 5 Hz, 1H), 7.84 (d, J = 5 Hz, 1H),
377 7.80–7.76 (m, 1H), 7.48 (d, J = 2.5 Hz, 1H), 7.40 (d, J = 10 Hz, 1H), 7.23–7.19 (m,
378 1H), 7.16–7.14 (m, 1H), 3.86 (s, 3H); ^{13}C NMR (125 MHz, $CDCl_3$) δ 157.9, 154.0,
379 148.1, 138.1, 137.5, 136.7, 135.6, 135.3, 130.2, 122.8, 121.4, 121.2, 118.3, 115.3,
380 112.6, 103.5, 55.9. IR (KBr, cm^{-1}) 3347, 1583, 1564, 1490, 1455, 1439, 1414, 1362,
381 1292, 1280, 1221, 1176, 1139, 1118, 1033, 1020, 837, 823, 798, 742, 630. Elemental
382 anal. calcd for $C_{17}H_{13}N_3O$: C, 74.17; H, 4.76; N, 15.26; found C, 74.15; H, 4.79; N,
383 15.30. HRMS (ESI) m/z calcd for $C_{17}H_{13}N_3O$ $[M+H]^+$ 276.1131, found 276.1128.

384 *4.2.1.7. 1-(benzo[d][1,3]dioxol-5-yl)-9H-pyrido[3,4-b]indole (**3g**)*: white solid; yield,
385 66%; m.p. 167.5–168.9 ^oC; ^1H NMR (500 MHz, $CDCl_3$) δ 8.63 (s, 1H), 8.57 (d, J = 5
386 Hz, 1H), 8.20 (d, J = 10 Hz, 1H), 7.95 (d, J = 5 Hz, 1H), 7.60 (t, J = 7.5 Hz, 1H), 7.55
387 (d, J = 10 Hz, 1H), 7.51–7.49 (m, 2H), 7.36 (t, J = 7.5 Hz, 1H), 7.05–7.03 (m, 1H),
388 6.09 (s, 2H); ^{13}C NMR (125 MHz, $CDCl_3$) δ 148.5, 148.2, 142.6, 140.3, 139.5, 133.31,
389 132.8, 129.8, 128.5, 122.0, 121.8, 120.3, 113.5, 111.5, 108.8, 108.7, 103.1, 101.4. IR
390 (KBr, cm^{-1}) 3054, 2884, 1626, 1565, 1502, 1471, 1452, 1415, 1320, 1283, 1243, 1223,
391 1126, 1039, 935, 919, 825, 812, 747. Elemental anal. calcd for $C_{18}H_{12}N_2O_2$: C, 74.99;
392 H, 4.20; N, 9.72; found C, 74.95; H, 4.18; N, 9.76. HRMS (ESI) m/z calcd for
393 $C_{18}H_{12}N_2O_2$ $[M+H]^+$ 289.0972, found 289.0970.

394 *4.2.1.8. 1-(benzo[d][1,3]dioxol-5-yl)-6-methoxy-9H-pyrido[3,4-b]indole (**3h**)*: yellow
395 solid; yield, 72%; m.p. 96.5–97.2 ^oC; ^1H NMR (500 MHz, $CDCl_3$) δ 8.91 (s, 1H), 8.44
396 (d, J = 5 Hz, 1H), 7.82 (d, J = 5 Hz, 1H), 7.54 (d, J = 5 Hz, 1H), 7.40–7.39 (m, 2H),
397 7.35 (d, J = 10 Hz, 1H), 7.17–7.16 (m, 1H), 6.87–6.86 (m, 1H), 5.94 (s, 2H), 3.92 (s,
398 3H); ^{13}C NMR (125 MHz, $CDCl_3$) δ 154.3, 148.4, 148.1, 142.9, 138.7, 135.5, 134.1,
399 132.7, 129.7, 122.3, 121.9, 118.5, 113.4, 112.5, 108.7,108.6, 103.5, 101.3, 56.0. IR
400 (KBr, cm^{-1}) 1565, 1501, 1470, 1447, 1285, 1248, 1209, 1158, 1113, 1038, 814.

Elemental anal. calcd for $C_{19}H_{14}N_2O_3$: C, 71.69; H, 4.43; N, 8.80; found C, 71.67; H, 4.41; N, 8.85. HRMS (ESI) m/z calcd for $C_{19}H_{14}N_2O_3$ $[M+H]^+$ 319.1077, found 319.1074.

*4.2.2. Synthesis of **4a–4x** and **5a–5i***

A solution of **3a**–**3h** (1 mmol) and substituted benzyl bromide (5 mmol) in acetonitrile (15 mL) was stirred at room temperature. The reaction was monitored by TLC. On completion, the resulting mixture was directly evaporated, and the residue was purified by silica gel column chromatography with dichloromethane and methanol (v/v = 20:1) to produce **4a**–**4h** and **5a**–**5i** in 67–96% yield.

*4.2.2.1. 2-benzyl-1-(4-(methoxycarbonyl)phenyl)-9H-pyrido[3,4-b]indol-2-ium bromide (**4a**)*: yellow solid; yield, 87%; m.p. 158.8–159.6 °C; ^{1}H NMR (500 MHz, CD_3OD) δ 8.82 (dd, J = 15 HZ, 5 Hz, 2H), 8.49 (d, J = 10 Hz, 1H), 8.27 (d, J = 10 Hz, 2H), 7.82–7.78 (m, 1H), 7.69–7.65 (m, 3H), 7.52–7.49 (m, 1H), 7.32–7.27 (m, 3H), 6.95–6.93 (m, 2H), 5.82 (s, 2H), 4.00 (s, 3H); ^{13}C NMR (125 MHz, CD_3OD) δ165.9, 145.2, 139.2, 135.8, 135.6, 134.4, 134.1, 132.8, 132.5, 132.4, 130.2, 130.0, 128.8, 128.6, 127.0, 123.1, 122.1, 119.8, 117.0, 112.6, 60.9, 51.7. IR (KBr, cm^{-1}) 3397, 3058, 2948, 1712, 1629, 1580, 1528, 1496, 1454, 1434, 1403, 1341, 1329, 1281, 1107, 1014, 767, 757, 705. Elemental anal. calcd for $C_{26}H_{21}BrN_2O_2$: C, 65.97; H, 4.47; N, 5.92; found C, 65.94; H, 4.51; N, 5.95. HRMS (ESI) m/z calcd for $C_{26}H_{21}BrN_2O_2$ $[M–Br]^+$ 393.1598, found 393.1592.

*4.2.2.2. 1-(4-(methoxycarbonyl)phenyl)-2-(4-methylbenzyl)-9H-pyrido[3,4-b]indol-2-ium bromide (**4b**)*: yellow solid; yield, 96%; m.p. 156.7–157.9 °C; ^{1}H NMR (500 MHz, CD_3OD) δ 8.82 (dd, J = 15 H_Z, 5 Hz, 2H), 8.47 (d, J = 10 Hz, 1H), 8.26 (d, J = 10 Hz, 2H), 7.81–7.77 (m, 1H), 7.67–7.63 (m, 3H), 7.51–7.48 (m, 1H), 7.31–7.27 (m, 2H), 6.95–6.93 (m, 2H), 5.82 (s, 2H), 4.00 (s, 3H), 2.27 (s, 3H); ^{13}C NMR (125 MHz, CD_3OD) δ 165.5, 143.3, 139.2, 135.7, 135.6, 134.4, 134.1, 132.6, 132.3, 132.1, 130.0, 129.7, 127.6, 125.9, 123.0, 121.7, 119.6, 118.8, 116.9, 112.6, 60.9, 50.9, 22.3. IR (KBr, cm^{-1}) 3401, 3016, 2950, 1720, 1605, 1587, 1531, 1505, 1464, 1442, 1401, 1327,

1275, 1108, 1010, 769, 756. Elemental anal. calcd for $C_{27}H_{23}BrN_2O_2$: C, 66.54; H, 4.76; N, 5.75; found C, 66.52; H, 4.77; N, 5.78. HRMS (ESI) m/z calcd for $C_{27}H_{23}BrN_2O_2$ $[M–Br]^+$ 407.1754, found 407.1754.

*4.2.2.3. 1-(4-(methoxycarbonyl)phenyl)-2-(4-(trifluoromethyl)benzyl)-9H-pyrido[3,4-b]indol-2-ium bromide (**4c**)*: yellow solid; yield, 92%; m.p. 159.2–160.3 ^oC; ^1H NMR (500 MHz, CD_3OD) δ 8.93 (d, J = 5 Hz, 1H), 8.87 (d, J = 10 Hz, 1H), 8.51 (d, J = 5 Hz, 1H), 8.28 (d, J = 10 Hz, 2H), 7.82 (t, J = 5 Hz, 1H), 7.76–7.74 (m, 2H), 7.69 (d, J = 10 Hz, 1H), 7.62 (d, J = 10 Hz, 2H), 7.52 (t, J = 7.5 Hz, 1H), 7.18 (d, J = 10 Hz, 2H), 5.99 (s, 2H), 4.02 (s, 3H); ^{13}C NMR (125 MHz, CD_3OD) δ 165.9, 145.3, 139.2, 138.8, 135.7, 134.4, 134.4, 133.0, 132.5, 132.4, 130.5, 130.3, 130.0, 127.7, 125.7, 125.6, 125.6, 125.6, 124.9, 123.2, 122.8, 122.1, 119.8, 117.3, 112.7, 60.3, 51.8. IR (KBr, cm^{-1}) 3347, 2360, 1581, 1565, 1490, 1455, 1439, 1414, 1362, 1291, 1280, 1221, 1176, 1139, 1119, 1090, 1034, 1020, 837, 824, 799, 768, 742, 701, 630, 543. Elemental anal. calcd for $C_{27}H_{20}BrF_3N_2O_2$: C, 59.90; H, 3.72; N, 5.17; found C, 59.87; H, 3.76; N, 5.12. HRMS (ESI) m/z calcd for $C_{27}H_{20}BrF_3N_2O_2$ $[M–Br]^+$ 461.1471, found 461.1469.

*4.2.2.4. 2-benzyl-6-methoxy-1-(4-(methoxycarbonyl)phenyl)-9H-pyrido[3,4-b]indol-2-ium bromide (**4d**)*: yellow solid; yield, 89%; m.p. 150.5–152.0 ^oC; ^1H NMR (500 MHz, DMSO-*d6*) δ 12.15 (s, 1H), 8.94 (t, J = 5 Hz, 2H), 8.18–8.16 (m, 2H), 8.11 (d, J = 5 Hz, 1H), 7.78 (d, J = 5 Hz, 2H), 7.59 (d, J = 10 Hz, 1H), 7.45–7.43 (m, 1H), 7.31–7.25 (m, 3H), 6.93 (d, J = 5 Hz, 2H), 5.80 (s, 2H), 3.95 (s, 3H), 3.92 (s, 3H); ^{13}C NMR (125 MHz, DMSO-*d6*) δ 166.1, 155.3, 140.6, 139.6, 136.0, 135.3, 134.1, 133.1, 133.0, 132.4, 131.0, 130.3, 129.2, 128.9, 127.6, 124.0, 120.5, 118.1, 114.6, 104.2, 60.5, 56.3, 53.1. IR (KBr, cm^{-1}) 3401, 1720, 1612, 1578, 1499, 1437, 1278, 1222, 1113, 1024, 821, 767, 738, 704. Elemental anal. calcd for $C_{27}H_{23}BrN_2O_3$: C, 64.42; H, 4.61; N, 5.57; found C, 64.40; H, 4.64; N, 5.56. HRMS (ESI) m/z calcd for $C_{27}H_{23}BrN_2O_3$ $[M–Br]^+$ 423.1703, found 423.1698.

*4.2.2.5. 6-methoxy-1-(4-(methoxycarbonyl)phenyl)-2-(4-methylbenzyl)-9H-pyrido[3,4-b]indol-2-ium bromide (**4e**)*: yellow solid; yield, 96%; m.p. 147.2–148.1 ^oC; ^1H NMR

(500 MHz, CD_3OD) δ 8.74 (dd, J = 10 Hz, 5 Hz, 2H), 8.27 (d, J = 10 Hz, 2H), 7.93 (d, J = 2.5 Hz, 1H), 7.68 (d, J = 10 Hz, 2H), 7.56 (d, J = 10 Hz, 1H), 7.45–7.42 (m, 1H), 7.11 (d, J = 5 Hz, 2H), 6.83 (d, J = 5 Hz, 2H), 5.74 (s, 2H), 4.01 (s, 3H), 3.97 (s, 3H), 2.30 (s, 3H); ^{13}C NMR (125 MHz, CD_3OD) δ 166.0, 155.8, 140.6, 139.3, 138.8, 135.7, 133.4, 133.1, 132.8, 132.6, 131.4, 130.2, 129.9, 129.4, 127.0, 124.1, 120.2, 117.0, 113.6, 102.6, 60.6, 55.0, 51.7, 19.7. IR (KBr, cm^{-1}) 3407, 3016, 2951, 1721, 1609, 1581, 1498, 1442, 1281, 1223, 1115, 1026, 826, 779, 707, 653. Elemental anal. calcd for $C_{28}H_{25}BrN_2O_3$: C, 65.00; H, 4.87; N, 5.41; found C, 64.97; H, 4.86; N, 5.44. HRMS (ESI) m/z calcd for $C_{28}H_{25}BrN_2O_3$ $[M–Br]^+$ 437.1860, found 437.1854.

*4.2.2.6. 6-methoxy-1-(4-(methoxycarbonyl)phenyl)-2-(4-(trifluoromethyl)benzyl)-9H-pyrido[3,4-b]indol-2-ium bromide (**4f**)*: yellow solid; yield, 81%; m.p. 168.7–169.6 ^{o}C; ^{1}H NMR (500 MHz, CD_3OD) δ 8.83 (s, 2H), 8.27 (d, J = 10 Hz, 2H), 7.94 (d, J = 2.5 Hz, 1H), 7.72 (d, J = 10 Hz, 2H), 7.60 (d, J = 10 Hz, 2H), 7.56 (d, J = 10 Hz, 1H), 7.42–7.39 (m, 1H), 7.16 (d, J = 5 Hz, 2H), 5.96 (s, 2H), 4.00 (s, 3H), 3.96 (s, 3H); ^{13}C NMR (125 MHz, CD_3OD) δ 167.3, 157.1, 142.0, 140.6, 140.3, 137.1, 135.0, 134.9, 134.3, 133.8, 131.9, 131.6, 131.4, 129.0, 127.0, 127.0, 126.9, 126.3, 125.5, 124.1, 121.6, 118.7, 115.0, 104.1, 61.5, 56.5, 53.1. IR (KBr, cm^{-1}) 3362, 3065, 2957, 1718, 1659, 1637, 1619, 1582, 1526, 1497, 1469, 1326, 1294, 1279, 1223, 1164, 1128, 1067, 1015, 870, 825, 792, 769, 726, 660, 645, 596. Elemental anal. calcd for $C_{28}H_{22}BrF_3N_2O_3$: C, 58.86; H, 3.88; N, 4.90; found C, 58.90; H, 3.87; N, 4.85. HRMS (ESI) m/z calcd for $C_{28}H_{22}BrF_3N_2O_3$ $[M–Br]^+$ 491.1577, found 491.1573.

*4.2.2.7. 2-benzyl-1-(furan-2-yl)-9H-pyrido[3,4-b]indol-2-ium bromide (**4g**)*: red-brown solid; yield, 83%; m.p. 141.1–142.7 ^{o}C; ^{1}H NMR (500 MHz, CD_3OD) δ 8.75–8.70 (m, 2H), 8.43 (d, J = 10 Hz, 1H), 8.12 (d, J = 2.5 Hz, 1H), 7.83–7.77 (m, 2H), 7.50–7.47 (m, 1H), 7.36–7.34 (m, 3H), 7.27 (d, J = 2.5 Hz, 1H), 7.13–7.11 (m, 2H), 6.88 (dd, J = 5 Hz, 2.5 Hz, 1H), 6.09 (s, 2H); ^{13}C NMR (125 MHz, CD_3OD) δ 148.7, 146.5, 141.8, 136.4, 136.1, 135.8, 135.7, 133.8, 130.8, 130.3, 130.0, 128.2, 124.3, 123.5, 121.1, 120.0, 118.2, 114.2, 113.9, 62.8. IR (KBr, cm^{-1}) 3399, 3055, 2924, 1627, 1580, 1500, 1453, 1335, 1270, 1249, 1201, 1153, 1018, 762, 742, 701.

Elemental anal. calcd for $C_{22}H_{17}BrN_2O$: C, 65.20; H, 4.23; N, 6.91; found C, 65.17; H, 4.25; N, 6.93. HRMS (ESI) m/z calcd for $C_{22}H_{17}BrN_2O$ $[M–Br]^+$ 325.1335, found 325.1332.

*4.2.2.8. 1-(furan-2-yl)-2-(4-methylbenzyl)-9H-pyrido[3,4-b]indol-2-ium bromide (**4h**)*: red-brown solid; yield, 85%; m.p. 156.6–157.8 ^oC; ^1H NMR (500 MHz, CD_3OD) δ 8.79–8.75 (m, 2H), 8.45 (d, J = 10 Hz, 1H), 8.08 (d, J = 2.5 Hz, 1H), 7.84–7.78 (m, 2H), 7.64 (d, J = 5 Hz, 2H), 7.50 (t, J = 5 Hz, 1H), 7.30–7.26 (m, 3H), 6.88–6.86 (m, 1H), 6.19 (s, 2H); ^{13}C NMR (125 MHz, CD_3OD) δ 149.1, 146.9, 141.9, 140.6, 136.7, 136.3, 134.3, 132.0, 131.1, 129.1, 127.4, 127.4, 124.8, 124.0, 121.5, 120.5, 118.7, 114.5, 114.3, 62.6, 31.0. IR (KBr, cm^{-1}) 3409, 3146, 3049, 2925, 2855, 1629, 1583, 1505, 1452, 1422, 1327, 1279, 1164, 1127, 1067, 1017, 753. Elemental anal. calcd for $C_{23}H_{19}BrN_2O$: C, 65.88; H, 4.57; N, 6.68; found C, 65.85; H, 4.59; N, 6.67. HRMS (ESI) m/z calcd for $C_{23}H_{19}BrN_2O$ $[M–Br]^+$ 339.1492, found 339.1490.

*4.2.2.9. 1-(furan-2-yl)-2-(4-(trifluoromethyl)benzyl)-9H-pyrido[3,4-b]indol-2-ium bromide (**4i**)*: red-brown solid; yield, 78%; m.p. 185.6–187.2 ^oC; ^1H NMR (500 MHz, CD_3OD) δ 8.80–8.75 (m, 2H), 8.45 (d, J = 2.5 Hz, 1H), 8.08 (s, 1H), 7.84–7.79 (m, 2H), 7.65 (d, J = 10 Hz, 2H), 7.50 (t, J = 5 Hz, 1H), 7.31–7.27 (m, 3H), 6.87 (dd, J = 12.5 Hz, 2.5 Hz, 1H), 6.2 (s, 2H); ^{13}C NMR (125 MHz, CD_3OD) δ 148.8, 146.6, 141.6, 140.2, 136.5, 136.4, 136.0, 134.0, 131.9, 131.7, 130.8, 128.7, 127.1, 127.1, 127.1, 127.0, 126.3, 124.4, 124.2, 123.6, 122.0, 121.2, 120.2, 118.4, 114.2, 114.0, 62.2. IR (KBr, cm^{-1}) 3410, 3048, 1629, 1511, 1502, 1327, 1280, 1164, 1127, 1067, 1018, 753. Elemental anal. calcd for $C_{23}H_{16}BrF_3N_2O$: C, 58.37; H, 3.41; N, 5.92; found C, 58.35; H, 3.43; N, 5.89. HRMS (ESI) m/z calcd for $C_{23}H_{16}BrF_3N_2O$ $[M–Br]^+$ 393.1209, found 393.1202.

*4.2.2.10. 2-benzyl-1-(furan-2-yl)-6-methoxy-9H-pyrido[3,4-b]indol-2-ium bromide (**4j**)*: red-brown solid; yield, 92%; m.p. 194.8–196.1 ^oC; ^1H NMR (500 MHz, DMSO-*d6*) δ 12.43 (s, 1H), 8.88 (dd, J = 10 Hz, 5 Hz, 2H), 8.24 (d, J = 2.5 Hz, 1H), 8.07 (d, J = 5 Hz, 1H), 7.73 (d, J = 10 Hz, 1H), 7.49–7.47 (m, 1H), 7.35–7.32 (m, 4H), 7.08–7.06 (m, 2H), 6.95 (dd, J = 5 Hz, 2.5 Hz, 1H), 6.07 (s, 2H), 3.92 (s, 3H); ^{13}C

NMR (125 MHz, DMSO-*d6*) δ155.1, 148.7, 146.5, 141.8, 136.4, 136.1, 135.8, 133.8, 130.8, 130.3, 130.0, 128.2, 124.3, 123.5, 121.1, 120.0, 118.2, 114.2, 113.9, 62.8, 56.4. IR (KBr, cm^{-1}) 3409, 3048, 2917, 1626, 1588, 1516, 1462, 1327, 1266, 1230, 1199, 1142, 1008, 767, 722. Elemental anal. calcd for $C_{23}H_{19}BrN_2O_2$: C, 63.46; H, 4.40; N, 6.44; found C, 63.45; H, 4.43; N, 6.40. HRMS (ESI) m/z calcd for $C_{23}H_{19}BrN_2O_2$ $[M–Br]^+$ 355.1441, found 355.1437.

*4.2.2.11. 1-(furan-2-yl)-6-methoxy-2-(4-methylbenzyl)-9H-pyrido[3,4-b]indol-2-ium bromide (**4k**)*: red-brown solid; yield, 81%; m.p. 191.6–193.2 ^oC; ^1H NMR (500 MHz, CD_3OD) δ 8.66 (dd, J = 10 Hz, 5 Hz, 2H), 8.10 (d, J = 5 Hz, 1H), 7.89 (d, J = 5 Hz, 1H), 7.69 (d, J = 10 Hz, 1H), 7.47–7.45 (m, 1H), 7.26 (d, J = 5 Hz, 1H), 7.16 (d, J = 5 Hz, 2H), 6.99 (d, J = 10 Hz, 2H), 6.88 (dd, J = 5 Hz, 2.5 Hz, 1H), 6.00 (s, 2H), 3.96 (s, 3H), 2.30 (s, 3H); ^{13}C NMR (125 MHz, CD_3OD) δ 157.3, 148.6, 141.9, 141.8, 140.2, 136.5, 135.1, 135.0, 132.8, 130.9, 128.2, 125.5, 121.6, 119.8, 118.1, 115.7, 115.2, 113.9, 104.0, 62.5, 56.4, 21.1. IR (KBr, cm^{-1}) 3424, 3047, 2998, 2953, 1632, 1605, 1582, 1512, 1498, 1469, 1434, 1351, 1311, 1295, 1221, 1184, 1126, 1023, 836, 807, 758. Elemental anal. calcd for $C_{24}H_{21}BrN_2O_2$: C, 64.15; H, 4.71; N, 6.23; found C, 64.19; H, 4.70; N, 6.19. HRMS (ESI) m/z calcd for $C_{24}H_{21}BrN_2O_2$ $[M–Br]^+$ 369.1598, found 369.1596.

*4.2.2.12. 1-(furan-2-yl)-6-methoxy-2-(4-(trifluoromethyl)benzyl)-9H-pyrido[3,4-b]indol-2-ium bromide (**4l**)*: red-brown solid; yield, 76%; m.p. 198.5–199.6 ^oC; ^1H NMR (500 MHz, CD_3OD) δ 8.72 (dd, J = 10 Hz, 5 Hz, 2H), 8.07 (d, J = 2.5 Hz, 1H), 7.92 (d, J = 2.5 Hz, 1H), 7.71–7.64 (m, 3H), 7.49–7.47 (m, 1H), 7.30–7.25 (m, 3H), 6.86 (dd, J = 5 Hz, 2.5 Hz, 1H), 6.17 (s, 2H), 3.97 (s, 3H); ^{13}C NMR (125 MHz, CD_3OD) δ 157.1, 148.5, 141.7, 141.4, 140.1, 136.3, 135.3, 135.0, 130.6, 128.4, 126.9, 126.8, 126.8, 126.8, 126.1, 125.4, 121.4, 120.7, 119.8, 118.2, 118.1, 115.0, 113.7, 103.7, 61.8, 56.2. IR (KBr, cm^{-1}) 3435, 3152, 3045, 1658, 1640, 1620, 1611, 1582, 1512, 1501, 1468, 1328, 1297, 1223, 1166, 1127, 1068, 1019. Elemental anal. calcd for $C_{24}H_{18}BrF_3N_2O_2$: C, 57.27; H, 3.60; N, 5.57; found C, 57.22; H, 3.65; N, 5.55. HRMS (ESI) m/z calcd for $C_{24}H_{18}BrF_3N_2O_2$ $[M–Br]^+$ 423.1315, found 423.1311.

*4.2.2.13. 2-benzyl-1-(pyridin-2-yl)-9H-pyrido[3,4-b]indol-2-ium bromide (**4m**)*: yellow solid; yield, 67%; m.p. 137.6–138.9 °C; ^{1}H NMR (500 MHz, DMSO-*d6*) δ 12.42 (s, 1H), 9.05–8.92 (m, 2H), 8.93–8.92 (m, 1H), 8.58 (d, *J* = 5 Hz, 1H), 8.12 (td, *J* = 5 Hz, 2.5Hz, 1H), 7.87 (d, *J* = 5 Hz, 1H), 7.82 (td, *J* = 5 Hz, 2.5Hz, 1H), 7.77–7.75 (m, 1H), 7.71 (d, *J* = 5 Hz, 1H), 7.50 (td, *J* = 10 Hz, 5Hz, 1H), 7.28–7.22 (m, 3H), 6.94 (dd, *J* = 10 Hz, 2.5 Hz, 2H), 5.97 (s, 2H); ^{13}C NMR (125 MHz, DMSO-*d6*) δ 150.6, 147.0, 144.8, 138.2, 137.3, 135.0, 134.7, 134.7, 133.9, 132.4, 128.6, 128.4, 127.2, 127.0, 126.0, 123.7, 121.9, 119.4, 117.9, 113.1, 59.9. IR (KBr, cm^{-1}) 3414, 3056, 2780, 1629, 1574, 1459, 1330, 1270, 1243, 745. Elemental anal. calcd for $C_{23}H_{18}BrN_3$: C, 66.36; H, 4.36; N, 10.09; found C, 66.33; H, 4.39; N, 10.12. HRMS (ESI) m/z calcd for $C_{23}H_{18}BrN_3$ $[M–Br]^+$ 336.1495, found 336.1494.

*4.2.2.14. 2-(4-methylbenzyl)-1-(pyridin-2-yl)-9H-pyrido[3,4-b]indol-2-ium bromide (**4n**)*: yellow solid; yield, 70%; m.p. 133.4–135.1 °C; ^{1}H NMR (500 MHz, CD_3OD) δ 8.95 (dt, *J* = 10 Hz, 2.5 Hz, 1H), 8.78 (dd, *J* = 10 Hz, 5 Hz, 2H), 8.45 (d, *J* = 5 Hz, 1H), 8.12 (td, *J* = 10 Hz, 2.5 Hz, 1H), 7.81–7.75 (m, 3H), 7.67 (d, *J* = 10 Hz, 1H), 7.48 (td, *J* = 10 Hz, 5 Hz, 1H), 7.07 (d, *J* = 10 Hz, 2H), 6.87 (d, *J* = 10 Hz, 2H), 5.90 (s, 2H), 2.26 (s, 3H); ^{13}C NMR (125 MHz, CD_3OD) δ 152.2, 148.7, 146.8, 140.2, 139.6, 138.7, 136.8, 136.1, 135.5, 133.9, 132.6, 130.7, 128.7, 128.2, 127.5, 124.5, 123.4, 121.0, 118.7, 114.0, 61.9, 21.1. IR (KBr, cm^{-1}) 3404, 3050, 3008, 2779, 1628, 1573, 1518, 1461, 1430, 1332, 1267, 1143, 793, 753. Elemental anal. calcd for $C_{24}H_{20}BrN_3$: C, 66.98; H, 4.68; N, 9.76; found C, 66.94; H, 4.71; N, 9.79. HRMS (ESI) m/z calcd for $C_{24}H_{20}BrN_3$ $[M–Br]^+$ 350.1652, found 350.1649.

*4.2.2.15. 1-(pyridin-2-yl)-2-(4-(trifluoromethyl)benzyl)-9H-pyrido[3,4-b]indol-2-ium bromide (**4o**)*: yellow solid; yield, 69%; m.p. 194.3–196.0 °C; ^{1}H NMR (500 MHz, CD_3OD) δ 8.91 (d, *J* = 5 Hz, 1H), 8.86 (dd, *J* = 10 Hz, 5 Hz, 2H), 8.50 (d, *J* = 10 Hz, 1H), 8.09 (td, *J* = 10 Hz, 2.5 Hz, 1H), 7.84–7.79 (m, 2H), 7.75–7.73 (m, 1H), 7.69 (d, *J* = 5 Hz, 1H), 7.56 (d, *J* = 5 Hz, 2H), 7.52 (t, *J* = 7.5 Hz, 1H), 7.18 (d, *J* = 10 Hz, 2H), 6.09 (s, 2H); ^{13}C NMR (125 MHz, CD_3OD) δ 152.2, 148.5, 146.9, 140.1, 139.6, 138.8, 136.9, 136.5, 135.9, 134.1, 131.9, 129.2, 128.3, 127.6, 126.9, 126.9, 126.9, 126.8,

126.3, 124.6, 124.1, 123.6, 121.1, 118.9, 114.1, 61.4. IR (KBr, cm^{-1}) 3347, 3011, 1629, 1330, 1274, 1165, 1112, 1067, 756. Elemental anal. calcd for $C_{24}H_{17}BrF_3N_3$: C, 59.52; H, 3.54; N, 8.68; found C, 59.49; H, 3.53; N, 8.71. HRMS (ESI) m/z calcd for $C_{24}H_{17}BrF_3N_3$ $[M–Br]^+$ 404.1369, found 404.1367.

*4.2.2.16. 2-benzyl-6-methoxy-1-(pyridin-2-yl)-9H-pyrido[3,4-b]indol-2-ium bromide (**4p**)*: yellow solid; yield, 79%; m.p. 157.2–158.6 °C; ^{1}H NMR (500 MHz, DMSO-*d6*) δ 8.99 (dd, *J* = 15 Hz, 5 Hz, 2H), 8.91 (d, *J* = 5 Hz, 1H), 8.13–8.10 (m, 2H), 7.87 (d, *J* = 5 Hz, 1H), 7.77–7.74 (m, 1H), 7.63 (d, *J* = 10 Hz, 1H), 7.44–7.42 (m, 1H), 7.27–7.21 (m, 3H), 6.94 (d, *J* = 5 Hz, 2H), 5.96 (s, 2H), 3.91 (s, 3H); ^{13}C NMR (125 MHz, DMSO-*d6*) δ 154.8, 150.6, 147.0, 140.3, 138.2, 137.4, 135.1, 134.7, 133.8, 133.2, 128.6, 128.4, 127.3, 127.0, 126.0, 123.6, 119.8, 117.8, 114.1, 103.8, 59.7, 55.8. IR (KBr, cm^{-1}) 3409, 3039, 2958, 1608, 1571, 1515, 1499, 1472, 1454, 1435, 1358, 1348, 1296, 1274, 1147, 1132, 1017, 824, 791, 730. Elemental anal. calcd for $C_{24}H_{20}BrN_3O$: C, 64.58; H, 4.52; N, 9.41; found C, 64.55; H, 4.54; N, 9.43. HRMS (ESI) m/z calcd for $C_{24}H_{20}BrN_3O$ $[M–Br]^+$ 366.1601, found 366.1593.

*4.2.2.17. 6-methoxy-2-(4-methylbenzyl)-1-(pyridin-2-yl)-9H-pyrido[3,4-b]indol-2-ium bromide (**4q**)*: yellow solid; yield, 75%; m.p. 164.8–165.6 °C; ^{1}H NMR (500 MHz, DMSO-*d6*) δ 12.30 (s, 1H), 8.96–8.93 (m, 3H), 8.17–8.12 (m, 2H), 7.90 (d, *J* = 10 Hz, 2.5 Hz, 1H), 7.79–7.76 (m, 1H), 7.63 (d, *J* = 10 Hz, 1H), 7.46–7.44 (m, 1H), 7.05 (d, *J* = 10 Hz, 2H), 6.85 (d, *J* = 10 Hz, 2H), 5.89 (s, 2H), 3.92 (s, 3H), 2.22 (s, 3H); ^{13}C NMR (125 MHz, DMSO-*d6*) δ 154.8, 150.6, 147.0, 140.1, 138.2, 137.9, 137.4, 135.0, 133.7, 133.1, 131.7, 129.2, 127.3, 127.0, 126.0, 123.6, 119.8, 117.8, 114.1, 103.8, 59.5, 55.8, 40.0, 39.8, 39.6, 39.5, 39.3, 39.1, 39.0, 20.6. IR (KBr, cm^{-1}) 3383, 3053, 3008, 1632, 1613, 1576, 1521, 1498, 1466, 1293, 1224, 1142, 1020, 825, 787. Elemental anal. calcd for $C_{25}H_{22}BrN_3O$: C, 65.22; H, 4.82; N, 9.13; found C, 65.20; H, 4.80; N, 9.17. HRMS (ESI) m/z calcd for $C_{25}H_{22}BrN_3O$ $[M–Br]^+$ 380.1757, found 380.1752.

*4.2.2.18. 6-methoxy-1-(pyridin-2-yl)-2-(4-(trifluoromethyl)benzyl)-9H-pyrido[3,4-b]indol-2-ium bromide (**4r**)*: yellow solid; yield, 70%; m.p. 144.8–145.7 °C; ^{1}H NMR

(500 MHz, CD_3OD) δ 8.89 (d, J = 5 Hz, 1H), 8.83 (dd, J = 10 Hz, 5 Hz, 2H), 8.37 (d, J = 10 Hz, 1H), 8.17 (td, J = 10 Hz, 2.5 Hz, 1H), 7.89–7.81 (m, 1H), 7.72–7.69 (m, 1H), 7.61 (d, J = 5 Hz, 1H), 7.47 (d, J = 5 Hz, 2H), 7.39 (t, J = 7.5 Hz, 1H), 7.18 (d, J = 10 Hz, 2H), 6.07 (s, 2H), 2.11 (s, 3H); ^{13}C NMR (125 MHz, CD_3OD) δ 153.4, 148.5, 146.8, 140.1, 139.6, 138.7, 137.0, 136.5, 135.9, 134.1, 131.9, 129.7, 128.0, 127.5, 127.1, 126.9, 126.9, 126.9, 126.6, 124.5, 124.0, 123.6, 121.0, 119.0, 114.2, 60.3, 20.1. IR (KBr, cm^{-1}) 3409, 3006, 2958, 1611, 1578, 1516, 1499, 1472, 1438, 1296, 1224, 1139, 792. Elemental anal. calcd for $C_{25}H_{19}BrF_3N_3O$: C, 58.38; H, 3.72; N, 8.17; found C, 58.34; H, 3.75; N, 8.20. HRMS (ESI) m/z calcd for $C_{25}H_{19}BrF_3N_3O$ $[M–Br]^+$ 434.1475, found 434.1470.

*4.2.2.19. 1-(benzo[d][1,3]dioxol-5-yl)-2-benzyl-9H-pyrido[3,4-b]indol-2-ium bromide (**4s**)*: yellow solid; yield, 83%; m.p. 152.8–153.4 ^{o}C; ^{1}H NMR (500 MHz, CD_3OD) δ 8.76–8.72 (m, 2H), 8.40 (d, J = 10 Hz, 1H), 7.75 (dd, J = 15 Hz, 5 Hz, 1H), 7.67 (d, J = 5 Hz, 1H), 7.67 (t, J = 5 Hz, 1H), 7.32–7.31 (m, 3H), 7.12 (d, J = 5 Hz, 1H), 7.08–7.03 (m, 4H), 6.16 (dd, J = 10 Hz, 2.5 Hz, 2H), 5.85 (s, 2H); ^{13}C NMR (125 MHz, CD_3OD) δ 151.9, 150.3, 146.3, 141.6, 137.3, 136.0, 135.2, 134.9, 133.4, 130.1, 129.9, 128.5, 125.6, 124.4, 123.2, 122.4, 121.2, 118.1, 114.0, 110.8, 110.4, 103.6, 61.9. IR (KBr, cm^{-1}) 3401, 3022, 2930, 1605, 1492, 1430, 1331, 1229, 1140, 1109, 1032, 767. Elemental anal. calcd for $C_{25}H_{19}BrN_2O_2$: C, 65.37; H, 4.17; N, 6.10; found C, 65.34; H, 4.15; N, 6.13. HRMS (ESI) m/z calcd for $C_{25}H_{19}BrN_2O_2$ $[M–Br]^+$ 379.1441, found 379.1439.

*4.2.2.20. 1-(benzo[d][1,3]dioxol-5-yl)-2-(4-methylbenzyl)-9H-pyrido[3,4-b]indol-2-ium bromide (**4t**)*: yellow solid; yield, 83%; m.p. 141.2–142.6 ^{o}C; ^{1}H NMR (500 MHz, CD_3OD) δ 8.73–8.67 (m, 2H), 8.40 (d, J = 5 Hz, 1H), 7.73 (t, J = 7.5 Hz, 1H), 7.65 (d, J = 5 Hz, 1H), 7.73 (t, J = 7.5 Hz, 1H), 7.14–7.12 (m, 3H), 7.09–7.07 (m, 1H), 7.04 (d, J = 2.5 Hz, 1H), 6.93 (d, J = 5 Hz, 2H), 6.18 (d, J = 10 Hz, 2H), 5.79 (s, 2H), 2.28 (s, 3H); ^{13}C NMR (125 MHz, CD_3OD) δ 151.9, 150.3, 146.3, 141.5, 140.1, 137.2, 135.1, 134.7, 133.4, 133.0, 130.7, 128.7, 125.6, 124.3, 123.2, 122.5, 121.2, 118.0, 114.0, 110.8, 110.4, 103.6, 61.7, 21.1. IR (KBr, cm^{-1}) 3387, 3012, 2921, 1627, 1482,

1434, 1334, 1233, 1144, 1113, 1033, 753. Elemental anal. calcd for $C_{26}H_{21}BrN_2O_2$: C, 65.97; H, 4.47; N, 5.92; found C, 65.95; H, 4.49; N, 5.90. HRMS (ESI) m/z calcd for $C_{26}H_{21}BrN_2O_2$ $[M–Br]^+$ 393.1598, found 393.1595.

*4.2.2.21. 1-(benzo[d][1,3]dioxol-5-yl)-2-(4-(trifluoromethyl)benzyl)-9H-pyrido[3,4-b]indol-2-ium bromide (**4u**)*: yellow solid; yield, 89%; m.p. 156.8–157.2 °C; ^{1}H NMR (500 MHz, CD_3OD) δ 8.82–8.79 (m, 2H), 8.44 (d, J = 10 Hz, 1H), 7.76 (t, J = 7.5 Hz, 1H), 7.68 (d, J = 10 Hz, 1H), 7.61 (d, J = 10 Hz, 2H), 7.45 (t, J = 7.5 Hz, 1H), 7.23 (d, J = 10 Hz, 1H), 7.11–7.05 (m, 3H), 6.15 (dd, J = 15 Hz, 2.5 Hz, 2H), 6.00 (s, 2H); ^{13}C NMR (125 MHz, CD_3OD) δ 157.1, 151.3, 150.2, 141.0, 139.5, 137.8, 135.0, 134.2, 131.4, 130.5, 129.1, 128.0, 127.8, 127.1, 126.8, 126.3, 124.9, 124.3, 123.9, 121.7, 121.7, 117.9, 114.8, 110.6, 110.2, 103.7, 102.6, 56.3. IR (KBr, cm^{-1}) 3402, 3015, 2780, 1628, 1484, 1435, 1325, 1236, 1166, 1118, 1065, 1036, 821, 753. Elemental anal. calcd for $C_{26}H_{18}BrF_3N_2O_2$: C, 59.22; H, 3.44; N, 5.31; found C, 59.19; H, 3.47; N, 5.34. HRMS (ESI) m/z calcd for $C_{26}H_{18}BrF_3N_2O_2$ $[M–Br]^+$ 447.1315, found 447.1313.

*4.2.2.22. 1-(benzo[d][1,3]dioxol-5-yl)-2-benzyl-6-methoxy-9H-pyrido[3,4-b]indol-2-ium bromide (**4v**)*: yellow solid; yield, 81%; m.p. 167.6–168.4 °C; ^{1}H NMR (500 MHz, CD_3OD) δ 8.68–8.63 (m, 2H), 7.90 (d, J = 2.5 Hz, 1H), 7.59 (d, J = 10 Hz, 1H), 7.45–7.42 (m, 1H), 7.34–7.32 (m, 3H), 7.10 (d, J = 5 Hz, 1H), 7.04–7.01(m, 4H), 6.15 (d, J = 5 Hz, 2H), 5.81 (s, 2H), 3.97 (s, 3H); ^{13}C NMR (125 MHz, CD_3OD) δ 157.2, 152.0, 150.3, 141.9, 141.8, 137.5, 136.2, 134.3, 134.3, 130.2, 129.9, 128.4, 125.5, 125.2, 122.5, 121.7, 118.0, 115.0, 110.7, 110.4, 104.0, 103.7, 61.7, 56.4. IR (KBr, cm^{-1}) 3394, 3060, 3023, 2955, 2903, 2836, 2790, 1609, 1580, 1487, 1443, 1344, 1313, 1248, 1223, 1156, 1112, 1033, 928, 819. Elemental anal. calcd for $C_{26}H_{21}BrN_2O_3$: C, 63.81; H, 4.33; N, 5.72; found C, 63.82; H, 4.30; N, 5.74. HRMS (ESI) m/z calcd for $C_{26}H_{21}BrN_2O_3$ $[M–Br]^+$ 409.1547, found 409.1544.

*4.2.2.23. 1-(benzo[d][1,3]dioxol-5-yl)-6-methoxy-2-(4-methylbenzyl)-9H-pyrido[3,4-b]indol-2-ium bromide (**4w**)*: yellow solid; yield, 88%; m.p. 166.5–167.2 °C; ^{1}H NMR (500 MHz, CD_3OD) δ 8.68–8.62 (m, 2H), 7.89 (d, J = 2.5 Hz, 1H), 7.58 (d, J =

2.5 Hz, 1H), 7.42–7.40(m, 1H), 7.16–7.03 (m, 5H), 6.92 (d, *J* = 10 Hz, 2H), 6.16 (d, *J* = 5 Hz, 2H), 5.76 (s, 2H), 3.95 (s, 3H), 2.30 (s, 3H); ^{13}C NMR (125 MHz, CD_3OD) δ 157.1, 151.9, 150.3, 141.8, 141.7, 140.1, 137.4, 134.2, 134.2, 133.1, 130.8, 128.5, 125.5, 125.1, 122.6, 121.7, 118.0, 115.0, 110.8, 110.4, 104.0, 103.7, 61.6, 56.4, 21.1. IR (KBr, cm^{-1}) 3442, 3058, 3025, 2963, 2892, 2835, 1612, 1578, 1523, 1485, 1439, 1344, 1317, 1299, 1224, 1188, 1113, 1038, 934, 822, 784. Elemental anal. calcd for $C_{27}H_{23}BrN_2O_3$: C, 64.42; H, 4.61; N, 5.57; found C, 64.39; H, 4.57; N, 5.60. HRMS (ESI) m/z calcd for $C_{27}H_{23}BrN_2O_3$ $[M–Br]^+$ 423.1703, found 423.1696.

*4.2.2.24. 1-(benzo[d][1,3]dioxol-5-yl)-6-methoxy-2-(4-(trifluoromethyl)benzyl)-9 H-pyrido[3,4-b]indol-2-ium bromide (**4x**)*: yellow solid; yield, 89%; m.p. 181.5–182.7 ^{o}C; ^{1}H NMR (500 MHz, CD_3OD) δ 8.72 (dd, *J* = 10 Hz, 5 Hz, 2H), 7.91 (d, *J* = 5 Hz, 1H), 7.64–7.58 (m, 3H), 7.43–7.41 (m, 1H), 7.20 (d, *J* = 5 Hz, 2H), 7.09–7.03 (m, 3H), 6.14 (d, *J* = 15 Hz, 2H), 5.95 (s, 2H), 3.96 (s, 3H); ^{13}C NMR (125 MHz, CD_3OD) δ 157.1, 152.0, 150.3, 141.9, 141.9, 140.6, 137.5, 134.6, 134.5, 131.8, 131.6, 129.0, 127.0, 127.0, 126.9, 126.9, 126.4, 125.5, 125.3, 124.2, 122.4, 121.7, 118.2, 115.0, 110.7, 110.4, 104.0, 103.7, 61.2, 56.4. IR (KBr, cm^{-1}) 3422, 3018, 2784, 1616, 1579, 1490, 1439, 1326, 1227, 1164, 1118, 1068, 1036, 936, 821. Elemental anal. calcd for $C_{27}H_{20}BrF_3N_2O_3$: C, 58.18; H, 3.62; N, 5.03; found C, 58.16; H, 3.59; N, 5.06. HRMS (ESI) m/z calcd for $C_{27}H_{20}BrF_3N_2O_3$ $[M–Br]^+$ 477.1421, found 477.1419.

*4.2.2.25. 2-(4-fluorobenzyl)-6-methoxy-1-(4-(methoxycarbonyl)phenyl)-9H-pyrido [3,4-b]indol-2-ium bromide (**5a**)*: yellow solid; yield, 73%; m.p. 158.9–156.3 ^{o}C; ^{1}H NMR (500 MHz, DMSO-*d6*) δ 12.18 (s, 1H), 8.93 (dd, *J* = 10 Hz, 5 Hz, 2H), 8.18 (d, *J* = 5 Hz, 2H), 8.10 (d, *J* = 2.5 Hz, 1H), 7.78 (d, *J* = 10 Hz, 2H), 7.58 (d, *J* = 10 Hz, 1H), 7.45–7.43 (m, 1H), 7.10 (t, *J* = 10 Hz, 2H), 7.00–6.97 (m, 2H), 5.78 (s, 2H), 3.95 (s, 3H), 3.92 (s, 3H); ^{13}C NMR (125 MHz, DMSO-*d6*) δ 165.6, 162.8, 160.8, 154.8, 140.2, 139.1, 135.5, 133.5, 132.5, 131.9, 131.0, 130.4, 129.9, 129.5, 123.5, 119.9, 117.5, 115.7, 114.1, 103.7, 59.4, 55.7, 52.6. IR (KBr, cm^{-1}) 3407, 3063, 2953, 1716, 1636, 1607, 1580, 1510, 1498, 1468, 1436, 1351, 1296, 1278, 1221, 1163, 1120, 1042, 1029, 1013, 825, 786, 762. Elemental anal. calcd for $C_{27}H_{22}BrFN_2O_3$: C, 62.20; H,

4.25; N, 5.37; found C, 62.17; H, 4.29; N, 5.34. HRMS (ESI) m/z calcd for $C_{27}H_{22}BrFN_2O_3$ $[M–Br]^+$ 441.1609, found 441.1605.

*4.2.2.26. 2-(4-chlorobenzyl)-6-methoxy-1-(4-(methoxycarbonyl)phenyl)-9H-pyrido [3,4-b]indol-2-ium chloride (**5b**)*: yellow solid; yield, 86%; m.p. 157.7–159.2 °C; ^{1}H NMR (500 MHz, DMSO-*d6*) δ 12.13 (s, 1H), 8.89 (s, 2H), 8.18 (d, J = 10 Hz, 2H), 8.08 (d, J = 2.5 Hz, 1H), 7.77 (d, J = 5 Hz, 2H), 7.60 (d, J = 10 Hz, 1H), 7.46–7.44 (m, 1H), 7.33 (d, J = 10 Hz, 2H), 7.33 (d, J = 5 Hz, 2H), 5.77 (s, 2H), 3.96 (s, 3H), 3.93 (s, 3H). IR (KBr, cm^{-1}) 3383, 3062, 2951, 2837, 1715, 1633, 1610, 1580, 1496, 1468, 1453, 1436, 1405, 1350, 1295, 1279, 1223, 1188, 1120, 1089, 1029, 1015, 826, 811, 782. Elemental anal. calcd for $C_{27}H_{22}Cl_2N_2O_3$: C, 65.73; H, 4.49; N, 5.68; found C, 65.71; H, 4.47; N, 5.70. HRMS (ESI) m/z calcd for $C_{27}H_{22}Cl_2N_2O_3$ $[M–Cl]^+$ 457.1313, 459.1284, found 457.1311, 459.1280.

*4.2.2.27. 2-(4-bromobenzyl)-6-methoxy-1-(4-(methoxycarbonyl)phenyl)-9H-pyrido [3,4-b]indol-2-ium bromide (**5c**)*: yellow solid; yield, 91%; m.p. 160.9–162.4 °C; ^{1}H NMR (500 MHz, DMSO-*d6*) δ 12.16 (s, 1H), 8.91 (dd, J = 10 Hz, 5 Hz, 2H), 8.19 (d, J = 5 Hz, 2H), 8.19 (d, J = 2.5 Hz, 1H), 7.79 (d, J = 10 Hz, 2H), 7.59 (d, J = 10 Hz, 1H), 7.48–7.44 (m, 3H), 6.90 (d, J = 10 Hz, 2H), 5.75 (s, 2H), 3.95 (s, 3H), 3.92 (s, 3H). IR (KBr, cm^{-1}) 3374, 3148, 3062, 2951, 1716, 1635, 1610, 1580, 1527, 1497, 1469, 1453, 1436, 1405, 1294, 1280, 1223, 1186, 1111, 1071, 1029, 1013, 826, 807, 782, 770. Elemental anal. calcd for $C_{27}H_{22}Br_2N_2O_3$: C, 55.69; H, 3.81; N, 4.81; found C, 55.67; H, 3.83; N, 4.78. HRMS (ESI) m/z calcd for $C_{27}H_{22}Br_2N_2O_3$ $[M–Br]^+$ 501.0808, 503.0788, found 501.0806, 503.0785.

*4.2.2.28. 2-(2-fluorobenzyl)-6-methoxy-1-(4-(methoxycarbonyl)phenyl)-9H-pyrido [3,4-b]indol-2-ium bromide (**5d**)*: yellow solid; yield, 72%; m.p. 155.8–156.9 °C; ^{1}H NMR (500 MHz, DMSO-*d6*) δ 12.18 (s, 1H), 8.94 (dd, J = 10 Hz, 5 Hz, 2H), 8.16 (d, J = 5 Hz, 2H), 8.11 (d, J = 2.5 Hz, 1H), 7.77 (d, J = 10 Hz, 2H), 7.59 (d, J = 10 Hz, 1H), 7.46–7.44 (m, 1H), 7.39–7.35 (m, 1H), 7.14–7.07 (m, 2H), 6.90 (t, J = 7.5 Hz, 1H), 5.88 (s, 2H), 3.95 (s, 3H), 3.92 (s, 3H); ^{13}C NMR (125 MHz, DMSO-*d6*) δ 165.6, 160.5, 158.5, 154.8, 140.2, 139.1, 135.4, 133.8, 132.7, 132.4, 131.9, 130.9, 130.9,

130.3, 129.8, 129.6, 129.6, 124.8, 123.6, 121.8, 121.7, 119.9, 117.4, 115.5, 115.3, 114.1, 103.7, 55.8, 54.9, 52.6. IR (KBr, cm^{-1}) 3409, 3046, 3015, 2954, 1723, 1608, 1580, 1497, 1454, 1439, 1295, 1278, 1225, 1183, 1119, 1102, 1028, 828, 764. Elemental anal. calcd for $C_{27}H_{22}BrFN_2O_3$: C, 62.20; H, 4.25; N, 5.37; found C, 62.17; H, 4.21; N, 5.41. HRMS (ESI) m/z calcd for $C_{27}H_{22}BrFN_2O_3$ $[M–Br]^+$ 441.1609, found 441.1597.

*4.2.2.29. 2-(3-fluorobenzyl)-6-methoxy-1-(4-(methoxycarbonyl)phenyl)-9H-pyrido [3,4-b]indol-2-ium bromide (**5e**)*: yellow solid; yield, 79%; m.p. 147.2–149.0 ^oC; ^1H NMR (500 MHz, DMSO-*d6*) δ 12.20 (s, 1H), 8.92 (t, *J* = 5 Hz, 2H), 8.17 (d, *J* = 10 Hz, 2H), 8.10 (d, *J* = 5 Hz, 1H), 7.78 (d, *J* = 10 Hz, 2H), 7.59 (d, *J* = 5 Hz, 1H), 7.46–7.43 (m, 1H), 7.33–7.29 (m, 1H), 7.13 (td, *J* = 10 Hz, 2.5 Hz, 1H), 6.83 (d, *J* = 10 Hz, 1H), 6.75 (d, *J* = 10 Hz, 1H), 5.80 (s, 2H), 3.95 (s, 3H), 3.92 (s, 3H). IR (KBr, cm^{-1}) 3397, 3006, 2952, 2835, 1722, 1635, 1611, 1579, 1526, 1498, 1467, 1452, 1437, 1403, 1348, 1279, 1223, 1184, 1131, 1118, 1030, 1013, 826, 779. Elemental anal. calcd for $C_{27}H_{22}BrFN_2O_3$: C, 62.20; H, 4.25; N, 5.37; found C, 62.18; H, 4.23; N, 5.39. HRMS (ESI) m/z calcd for $C_{27}H_{22}BrFN_2O_3$ $[M–Br]^+$ 441.1609, found 441.1607.

*4.2.2.30. 2-(2-bromobenzyl)-6-methoxy-1-(4-(methoxycarbonyl)phenyl)-9H-pyrido [3,4-b]indol-2-ium bromide (**5f**)*: yellow solid; yield, 93%; m.p. 249.8–251.1 ^oC; ^1H NMR (500 MHz, DMSO-*d6*) δ 12.21 (s, 1H), 8.94–8.81 (m, 2H), 8.15 (d, *J* = 10 Hz, 2H), 8.11 (d, *J* = 2.5 Hz, 1H), 7.76 (d, *J* = 10 Hz, 2H), 7.61–7.58 (m, 2H), 7.48–7.45 (m, 1H), 7.32–7.26 (m, 2H), 6.84 (d, *J* = 5 Hz, 1H), 5.81 (s, 2H), 3.93 (s, 3H), 3.93 (s, 3H). IR (KBr, cm^{-1}) 3009, 2986, 2951, 1720, 1608, 1577, 1496, 1437, 1297, 1268, 1229, 1133, 1118, 1104, 1029, 828, 765. Elemental anal. calcd for $C_{27}H_{22}Br_2N_2O_3$: C, 55.69; H, 3.81; N, 4.81; found C, 55.66; H, 3.84; N, 4.79. HRMS (ESI) m/z calcd for $C_{27}H_{22}Br_2N_2O_3$ $[M–Br]^+$ 501.0808, 503.0788, found 501.0806, 503.0785.

*4.2.2.31. 2-(3-bromobenzyl)-6-methoxy-1-(4-(methoxycarbonyl)phenyl)-9H-pyrido [3,4-b]indol-2-ium bromide (**5g**)*: yellow solid; yield, 95%; m.p. 150.3–152.1 ^oC; ^1H NMR (500 MHz, DMSO-*d6*) δ 12.19 (s, 1H), 8.93 (dd, *J* = 10 Hz, 5 Hz, 2H), 8.17 (d, *J* = 10 Hz, 2H), 8.09 (d, *J* = 5 Hz, 1H), 7.76 (d, *J* = 10 Hz, 2H), 7.58 (d, *J* = 10 Hz,

1H), 7.49–7.43 (m, 2H), 7.21 (t, *J* = 7.5 Hz, 1H), 7.13 (t, *J* = 2.5 Hz, 1H), 6.91 (d, *J* = 10 Hz, 1H), 5.79 (s, 2H), 3.95 (s, 3H), 3.92 (s, 3H). IR (KBr, cm^{-1}) 3409, 3046, 3015, 2954, 2837, 1723, 1608, 1580, 1497, 1454, 1439, 1349, 1295, 1279, 1225, 1183, 1151, 1133, 1119, 1102, 1028, 1012, 828, 764. Elemental anal. calcd for $C_{27}H_{22}Br_2N_2O_3$: C, 55.69; H, 3.81; N, 4.81; found C, 55.67; H, 3.84; N, 4.83. HRMS (ESI) m/z calcd for $C_{27}H_{22}Br_2N_2O_3$ $[M–Br]^+$ 501.0808, 503.0788, found 501.0807, 503.0786.

*4.2.2.32. 2-(2,4-difluorobenzyl)-6-methoxy-1-(4-(methoxycarbonyl)phenyl)-9H-pyrido[3,4-b]indol-2-ium bromide (**5h**)*: yellow solid; yield, 87%; m.p. 142.3–144.3 ^oC; ^1H NMR (500 MHz, DMSO-*d6*) δ 12.14 (s, 1H), 8.93 (dd, *J* = 10 Hz, 5 Hz, 2H), 8.19 (d, *J* = 5 Hz, 2H), 8.10 (d, *J* = 2.5 Hz, 1H), 7.78 (d, *J* = 10 Hz, 2H), 7.58 (d, *J* = 5 Hz, 1H), 7.46–7.44 (m, 1H), 7.23–7.19 (m, 1H), 7.02–6.96 (m, 2H), 5.84 (s, 2H), 3.96 (s, 3H), 3.92 (s, 3H). IR (KBr, cm^{-1}) 3069, 3034, 3002, 2960, 1711, 1609, 1577, 1532, 1501, 1472, 1435, 1409, 1318, 1286, 1227, 1184, 1136, 1110, 1086, 1035, 1014, 960, 827, 767. Elemental anal. calcd for $C_{27}H_{21}BrF_2N_2O_3$: C, 60.12; H, 3.92; N, 5.19; found C, 60.15; H, 3.90; N, 5.15. HRMS (ESI) m/z calcd for $C_{27}H_{21}BrF_2N_2O_3$ $[M–Br]^+$ 459.1515, found 459.1513.

*4.2.2.33. 6-methoxy-1-(4-(methoxycarbonyl)phenyl)-2-(4-nitrobenzyl)-9H-pyrido[3,4-b]indol-2-ium chloride (**5i**)*: yellow solid; yield, 83%; m.p. 162.1–162.8 ^oC; ^1H NMR (500 MHz, DMSO-*d6*) δ 12.34 (s, 1H), 9.01 (dd, *J* = 10 Hz, 5 Hz, 2H), 8.15–8.12 (m, 5H), 7.78 (d, *J* = 5 Hz, 2H), 7.64 (d, *J* = 10 Hz, 1H), 7.50–7.47 (m, 1H), 7.23 (d, *J* = 10 Hz, 2H), 6.00 (s, 2H), 3.97 (s, 3H), 3.96 (s, 3H); ^{13}C NMR (125 MHz, DMSO-*d6*) δ 165.5, 154.8, 147.1, 142.3, 139.3, 137.0, 135.7, 133.7, 133.6, 132.9, 132.7, 132.4, 131.9, 130.4, 129.8, 128.1, 123.6, 120.0, 117.6, 103.6, 59.3, 55.7, 52.5. IR (KBr, cm^{-1}) 2998, 2952, 1715, 1610, 1580, 1522, 1500, 1434, 1405, 1345, 1318, 1285, 1229, 1135, 1110, 829. Elemental anal. calcd for $C_{27}H_{22}ClN_3O_5$: C, 64.35; H, 4.40; N, 8.34; found C, 64.31; H, 4.42; N, 8.33. HRMS (ESI) m/z calcd for $C_{27}H_{22}ClN_3O_5$ $[M–Cl]^+$ 468.1554, found 468.1551.

*4.2.3. X-ray structures of compounds **3e** and **5f***

X-ray quality crystal of compound **3e** was obtained from the dichloromethane: petroleum ether = 4:1 solution after 3 days. The crystal structure of compound **3e** (Fig. 4) was determined on a Rigaku Oxford Diffraction Supernova Dual Source at 100 K, Cu at Zero equipped with an AtlasS2 CCD using Cu Kα radiation. The atomic coordinates have been deposited at the Cambridge Crystallographic Data Center (CCDC) with CCDC numbers 1819364. It is worth mentioning that this crystal structure has been published earlier [39].

X-ray quality crystal of compound **5f** was obtained from the dichloromethane: methanol = 2:1 solution after 3 days. The crystal structure of compound **5f** (Fig. 4) was determined on a Rigaku Oxford Diffraction Supernova Dual Source at 100 K, Cu at Zero equipped with an AtlasS2 CCD using Cu Kα radiation. The atomic coordinates have been deposited at the Cambridge Crystallographic Data Center (CCDC) with CCDC numbers 1819367.

4.3. Antibacterial assay

MICs were determined as described by the National Committee for Clinical Laboratory Standards [40]. Four Gram-positive bacteria (*S. aureus*, MRSA, *B. cereus*, and *B. subtilis*) and two Gram-negative bacteria (*E. coli* and *R. solanacearum*) were selected as the tested bacteria. *S. aureus* 1.8721, *B. cereus* 1.1846 and and *Escherichia coli* 1.1636 were purchased from the China General Microbiological Culture Collection Center. MRSA (*S. aureus* ATCC 43300) and *B. subtillis* 769 were provided by College of Chemistry & Pharmacy, Northwest A&F University. *R. solanacearum* (CGMCC 1.12711) was provided by the College of Plant Protection, Northwest A&F University. The MIC was defined as the minimum inhibitory concentration, each compound resulting in visible inhibition on bacteria growth (incubation at 37 °C for 12–14 h). Each bacterial suspension was adjusted to a concentration of 1×10^6 CFU/mL. All compounds were thoroughly dried before weighing. Initially, the compounds were dissolved in dimethyl sulfoxide (DMSO) to prepare the stock solutions. The tested compounds and reference drugs were then prepared in liquid Luria–Bertan media. The required concentrations were 200, 100, 50, 25, 12.5, 6.25

and 3.125 nmol/mL, respectively (DMSO < 0.5%). Their MICs of the preferred compounds **4f**, **4i**, **4l**, **4u**, **4w**, **4x**, **5c** and reference drugs were also tested at concentrations of 256, 128, 64, 32, 16, 8, 4, 2 and 1 μg/mL.

4.4. Cell toxicity

The cytotoxicity of compounds **4f**, **4i**, **4l**, **4u**, **4w**, **4x** and **5c** was assessed using the 3-(4,5-dimethyl-2-thiazolyl)-2,5-diphenyl-2-H-tetrazolium bromide (MTT) assay, as described previously [41]. MARC 145 cells and L02 cells were treated with compounds **4f**, **4i**, **4l**, **4u**, **4w**, **4x** and **5c** at concentrations of 8 μg/mL. After incubation, 10 μL (5 mg/mL) of MTT in phosphate-buffered saline was added to each well, and the cells were incubated in 5% CO_2 at 37 °C for 4 h. The medium was removed. Then the DMSO (150 μL) was added to each well. The wells were shocked for 15 min in a flat shaker to dissolve purple formazan crystals. Finally, the plate was tested at 540 nm. The untreated group was considered as the control. The data were analyzed by GraphPad Prism 6.0. The formula used for cell viability was (absorbance of compound-treated cells/absorbance of untreated cells) × 100%.

4.5. Calculation of molecular physicochemical properties

Molecular properties, including the octanol–water partition coefficient, the topological polar surface area, the number of hydrogen bond acceptors, the number of hydrogen bond donors, the number of rotatable bonds, and the molecular volume, were calculated using the Molinspiration tool [42].

4.6. Thermal stability assay in vitro

The thermal stability assay *in vitro* used the UHPLC-ESI-MS/MS method [43]. A Nexera UHPLC LC-30A instrument was coupled to an AB SCIEX Triple TOF 5600^+ spectrometer. During experiments, a 5 μL (2 μg/mL for ampicillin sodium, 1 μg/mL for **4x**) sample was loaded along with mobile phase A (10% acetonitrile in double-distilled water for ampicillin sodium, 35% acetonitrile in double-distilled water for **4x**) at a flow rate of 0.4 mL/min. A sweeping collision energy setting of 35 ± 15 eV was applied to all precursor ions for collision-induced dissociation. The mass

spectrometer settings used varied, depending on the optimization required, but typical values were GS 1 = 50, GS 2 = 50, CUR = 35, and TEM = 500. The negative ion mode (–4500 V) was used for ampicillin sodium, and the positive ion mode (5500 V) was used for compound **4x**. The stability study was tested under three conditions (25 °C, 0 h; 37 °C, 6 h; 65 °C, 6 h).

4.7. SEM assay

A standard procedure was followed for SEM analysis [44]. Briefly, bacterial broth cultures in the log phase (30 mL) at ~10^8 CFU/mL were treated with freshly prepared phosphate-buffered saline (0.1 M, pH 7.2) in combination with 1 h of incubation at 37 °C. All samples were centrifuged at 4000 × *g* for 10 min, washed, and resuspended in phosphate-buffered saline. Bacterial cells were fixed with 2.5% glutaraldehyde, and then incubated at 37 °C on a glass slide (22 × 22 mm) for 20 min. Samples were dehydrated by passing through gradient ethanol (10%, 30%, 50%, 70%, 90%, and 100%) for 5 min at each concentration. Slides were then dried with an automatic critical point drying instrument (Leica EM CPD300), and a small amount of gold was sputtered onto the samples using a sputter coater system to avoid charging in the microscope. The treated group, with compound **4x** (0.5 MIC) added, was incubated at 37 °C for 1 h.

4.8. Molecular docking study

Molecular docking evaluation was conducted using the Surflex-Dock program in the Sybyl-X 2.0 package and Discovery Studio 2017 client. The crystal structures of bacterial type II topoisomerase (PDB ID: 5IWM) and type I topoisomerase (PDB ID: 4RUL) were obtained from the Protein Data Bank (http://www.pdb.org). The crystal structures of topoisomerases were prepared with all hydrogen atoms added, and charge added by the AMBER7 FF99 method. The structures of **4x** and ciprofloxacin were drawn in the Sybyl-X 2.0 package. Polar hydrogen atoms were then added, and the energy optimized with the Tripos force field and by the Gasteiger–Hückel method.

4.9. Antibacterial assay in vivo[37,38]

The *in vivo* biological assay against *R. solanacearum* for the compound **4x** was carried out on an eggplant leaf. The concentration of compound **4x** was 8 μg/mL (5‰ DMSO in water as the solvent). The blank control was 5‰ aqueous DMSO. Each suspension (V = 100 μL) was dropped onto the leaf of eggplant, which was washed and treated with water and 75% aqueous ethyl alcohol in advance. After the solvent was evaporated in an ambient environment, the epidermis (Ø 4.5 mm) of the leaf was punctured with an inoculating needle, and the pathogen then inoculated. All the treated leaves were placed in an illumination incubator (37 °C, 100% relative humidity, light/dark = 10 h/14 h) for 3 days, and the experiments were repeated three times.

Acknowledgements

This work was financially supported by the National Natural Science Foundation of China (Grant No. 81773603), the Open Foundation of Key Laboratory of Synthetic and Natural Functional Molecule Chemistry of Ministry of Education (Northwest University, China), and the State Key Laboratory of Drug Research (Grant No. SIMM1705KF-09).

Appendix A. Supplementary data

Supplementary data related to this article can be found.

Conflict of interest

The authors state no conflict of interest.

References

[1] B. S. Moore, G. T. Carter, M. Bronstrup, Editorial: Are natural products the solution to antimicrobial resistance?, Nat. Prod. Rep. 34 (2017) 685–686.

[2] R. Laxminarayan, A. Duse, C. Wattal, A. K. M. Zaidi, H. F. L. Wertheim, N. Sumpradit, E. Vlieghe, G. L. Hara, I. M. Gould, H. Goossens, C. Greko, A. D. So, M. Bigdeli, G. Tomson, W. Woodhouse, E. Ombaka, A. Q. Peralta, F. N. Qamar, F. Mir, S. Kariuki, Z. A. Bhutta, A. Coates, R. Bergstrom, G. D. Wright, E. D. Brown, O. Cars, Antibiotic resistance-the need for global solutions,

888 Lancet. Infect. Dis. 13 (2013) 1057–1098.

889 [3] V. Economou, P. Gousia, Agriculture and food animals as a source of antimicrobial-resistant
890 bacteria, Infect. Drug Resist. 8 (2015) 49–61.

891 [4] P. Widsten, C. D. Cruz, G. C. Fletcher, M. A. Pajak, T. K. McGhie, Tannins and extracts of
892 fruit byproducts: antibacterial activity against foodborne bacteria and antioxidant capacity, J. Agr.
893 Food. Chem. 62 (2014) 11146–11156.

894 [5] C. Pal, J. Bengtsson-Palme, E. Kristiansson, D. G. J. Larsson, The structure and diversity of
895 human, animal and environmental resistomes, Microbiome 4 (2016) 54.

896 [6] T. R. Walsh, J. Efthimiou, B. Dréno, Systematic review of antibiotic resistance in acne: an
897 increasing topical and oral threat, Lancet. Infect. Dis. 16 (2016) e23–e33.

898 [7] O. Genilloud, Actinomycetes: still a source of novel antibiotics, Nat. Prod. Rep. 34 (2017)
899 1203–1232.

900 [8] J. O'Neill, Tackling drug-resistant infections globally: final report and recommendations.
901 Review on antimicrobial resistance, (2016) Government of the UK. http://apo.org.au/node/63983.

902 [9] M. Antoszczak, K. Popiel, J. Stefańska, J. Wietrzyk, E. Maj, J. Janczak, G. Michalska, B.
903 Brzezinski, A. Huczyński, Synthesis, cytotoxicity and antibacterial activity of new esters of
904 polyether antibiotic–salinomycin, Eur. J. Med. Chem. 76 (2014) 435–444.

905 [10] G. Nenaah, Antibacterial and antifungal activities of (beta)-carboline alkaloids of *Peganum*
906 *harmala* (L) seeds and their combination effects, Fitoterapia 81 (2010) 779–782.

907 [11] G. O'Donnell, S. Gibbons, Antibacterial activity of two canthin-6-one alkaloids from *Allium*
908 *neapolitanum*, Phytother. Res. 21 (2007) 653–657.

909 [12] C. M. Roggero, J. M. Giulietti, S. P. Mulcahy, Efficient synthesis of eudistomin U and
910 evaluation of its cytotoxicity, Bioorg. Med. Chem. Lett. 24 (2014) 3549–3551.

911 [13] J. K. Dai, W. J. Dan, N. Li, H. T. Du, J. W. Zhang, J. R. Wang, Synthesis, *in vitro* antibacterial
912 activities of a series of 3-*N*-substituted canthin-6-ones, Bioorg. Med. Chem. Lett. 26 (2016) 580–
913 583.

914 [14] J. W. Zhang, L. B. Li, W. J. Dan, J. Li, Q. L. Zhang, H. J. Bai, J. R. Wang, Synthesis and
915 antimicrobial activities of 3-methyl-*β*-carboline derivatives, Nat. Prod. Commun. 10 (2015) 899–
916 902.

917 [15] R. N. Rao, B. Maiti, K. Chanda, Application of pictet-spengler reaction to indole-based

alkaloids containing tetrahydro-*β*-carboline scaffold in combinatorial chemistry, ACS Comb. Sci. 19 (2017) 199–228.

[16] H. J. Song, Y. X. Liu, Y. X. Liu, L. Z. Wang, Q. M. Wang, Synthesis and antiviral and fungicidal activity evaluation of *β*-carboline, dihydro-*β*-carboline, tetrahydro-*β*-carboline alkaloids, and their derivatives, J. Agr. Food. Chem. 62 (2014) 1010–1018.

[17] H. T. Du, H. L. Gu, N. Li, J. R. Wang, Synthesis and biological evaluation of bivalent *β*-carbolines as potential anticancer agents, MedChemComm 7 (2016) 636–645.

[18] A. R. Benoit, C. Schiaffo, C. E. Salomon, J. R. Goodell, H. Hiasa, D. M. Ferguson, Synthesis and evaluation of *N*-alkyl-9-aminoacridines with antibacterial activity, Bioorg. Med. Chem. Lett. 24 (2014) 3014–3017.

[19] M. W. Griffiths, H. Schraft, Chapter 20 – *Bacillus cereus* food poisoning. Foodborne Diseases (Third edition) (2017) 395–405.

[20] M. Salanoubat, S. Genin, F. Artiguenave, C. A. Boucher, Genome sequence of the plant pathogen *Ralstonia solanacearum*, Nature 415 (2002) 497–502.

[21] L. C. Meurer, R. N. Guthikonda, J. L. Huber, F. DiNinno, The synthesis and antibacterial activity of 2-carbolinyl-carbapenems: potent anti-MRSA/MRCNS agents, Bioorg. Med. Chem. Lett. 5 (1995) 767–772.

[22] Q. K. Shen, C. F. Liu, H. J. Zhang, Y. S. Tian, Z. S. Quan, Design and synthesis of new triazoles linked to xanthotoxin for potent and highly selective anti-gastric cancer agents, Bioorg. Med. Chem. Lett. 27 (2017) 4871–4875.

[23] Q. B. Xu, X. F. Chen, J. Feng, J. F. Miao, J. Liu, F. T. Liu, B. X. Niu, J. Y. Cai, C. Huang, Y. N. Zhang, Y. Ling, Design, synthesis and biological evaluation of hybrids of *β*-carboline and salicylic acid as potential anticancer and apoptosis inducing agents, Sci. Rep. 6 (2016) 36238.

[24] S. F. Cui, D. Addla, C. H. Zhou, Novel 3-aminothiazolquinolones: design, synthesis, bioactive evaluation, SARs, and preliminary antibacterial mechanism, J. Med. Chem. 59 (2016) 4488–4510.

[25] C. A. Lipinski, F. Lombardo, B. W. Dominy, P. J. Feeney, Experimental and computational approaches to estimate solubility and permeability in drug discovery and development settings, Adv. Drug Deliver. Rev. 23 (1997) 3–25.

[26] E. D. Clarke, J. S. Delaney, Physical and molecular properties of agrochemicals: an analysis

of screen inputs, hits, leads, and products, Chimia 57 (2003) 731–734.

[27] W. Hou, G. J. Zhang, Z. Luo, D. Li, H. Q. Quan, B. H. Ruan, L. Su, H. T. Xu, Identification of a diverse synthetic abietane diterpenoid library and insight into the structure–activity relationships for antibacterial activity, Bioorg. Med. Chem. Lett. 27 (2017) 5382–5386.

[28] Z. Q. Luo, X. J. Chen, G. P. Wang, Z. B. Du, X. Y. Ma, H. Wang, G. H. Yu, A. X. Liu, M. W. Li, W. Peng, Y. Liu, Development of a validated HPLC method for the quantitative determination of trelagliptin succinate and its related substances in pharmaceutical dosage forms, Eur. J. Pharm. Sci. 111 (2018) 458–464.

[29] N. S. Abdelwahab, M. T. Elsaady, A. G. Korany, M. A. Hegazy, Study of gliquidone degradation behavior by high–performance thin–layer chromatography and ultra–performance liquid chromatography methods, Biomed. Chromatogr. 31 (2017) e4025.

[30] T. A. Pham, A. N. Jain, Parameter estimation for scoring protein-ligand interactions using negative training data, J. Med. Chem. 49 (2006) 5856–5868.

[31] A. N. Jain, Scoring noncovalent protein-ligand interactions: A continuous differentiable function tuned to compute binding affinities, J. Comput. Aid. Mol. Des. 10 (1996) 427–440.

[32] A. M. L. Hossion, Y. Zamami, R. K. Kandahary, T. Tsuchiya, W. Ogawa, A. Iwado, K. Sasaki, Quercetin diacylglycoside analogues showing dual inhibition of DNA gyrase and topoisomerase IV as novel antibacterial agents, J. Med. Chem. 54 (2011) 3686–3703.

[33] J. Kovvuri, B. Nagaraju, V. L. Nayak, R. Akunuri, M.P. N. Rao, A. Ajitha, N. Nagesh, A. Kamal, Design, synthesis and biological evaluation of new β-carboline-bisindole compounds as DNA binding, photocleavage agents and topoisomerase I inhibitors, Eur. J. Med. Chem. 143 (2018) 1563–1577.

[34] B. Kramer, M. Rarey, T. Lengauer, Evaluation of the FlexX incremental construction algorithm for protein-ligand docking, Proteins 37 (1999) 228–241.

[35] M. Kontoyianni, L. M. McClellan, G. S. Sokol, Evaluation of docking performance: Comparative data on docking algorithms, J. Med. Chem. 47 (2004) 558–565.

[36] H. Jiang, W. Zhang, P. Li, J. Wang, C. Dong, K. Zhang, H. Chen, Z. Du, Synthesis and biological evaluation of novel carbazole-rhodanine conjugates as topoisomerase II inhibitors, Bioorg. Med. Chem. Lett. 28 (2018) 1320–1323.

[37] P. Li, L. Shi, X. Yang, L. Yang, X. W. Chen, F. Wu, Q. C. Shi, W. M. Xu, M. He, D. Y. Hu, B.

978 A. Song, Design, synthesis, and antibacterial activity against rice bacterial leaf blight and leaf
979 streak of 2,5-substituted-1,3,4-oxadiazole/thiadiazole sulfone derivative, Bioorg. Med. Chem. Lett.
980 24 (2014) 1677–1680.
981 [38] D. D. Li, S. S. Zhang, Z. H. Zong, G. T. Wang, S. K. Li, Bioactivity-guided mixed synthesis
982 accelerate the serendipity in lead optimization: Discovery of fungicidal homodrimanyl amides, Eur.
983 J. Med. Chem. 136 (2017) 114–121.
984 [39] C. P. Tan, S. S. Lai, S. H. Wu, S. Hu, L. J. Zhou, Y. Chen, M. X. Wang, Y. P. Zhu, W. Lian, W.
985 L. Peng, L. N. Ji, A. L. Xu, Nuclear permeable ruthenium(II) *β*-carboline complexes induce
986 autophagy to antagonize mitochondrial-mediated apoptosis, J. Med. Chem. 53 (2010) 7613–7624.
987 [40] *Performance Standards for Antimicrobial Susceptibility Testing; 11th Informational*
988 *Supplement*; National Committee for Clinical Laboratory Standards: Wayne, PA; Vol. 21, No. 1,
989 M100–S11.
990 [41] H. T. Du, S. Tian, J. C. Chen, H. L. Gu, N. Li, J. R. Wang, Synthesis and biological
991 evaluation of N^9-substituted harmine derivatives as potential anticancer agents, Bioorg. Med.
992 Chem. Lett. 26 (2016) 4015–4019.
993 [42] Molinspiration Cheminformatics, Cheminformatics on the Web. www.molinspiration.com.
994 [43] A. Vidal, V. Sanchis, A. J. Ramos, S. Marín, Thermal stability and kinetics of degradation of
995 deoxynivalenol, deoxynivalenol conjugates and ochratoxin A during baking of wheat bakery
996 products, Food Chem. 178 (2015) 276–286.
997 [44] R. Sharma, S. Patel, C. Abboud, J. Diep, N. S. Ly, J. M. Pogue, K. S. Kaye, J. Li, G. G. Rao,
998 Polymyxin B in combination with meropenem against carbapenemase-producing Klebsiella
999 pneumoniae: pharmacodynamics and morphological changes. Int. J. Antimicrob. Ag. 49 (2017)
1000 224–232.

Table Captions

Table 1. *In vitro* antibacterial activity of compounds **3a**–**3h** and **4a**–**4x** (MIC, nmol/mL).

Table 2. *In vitro* antibacterial activity of compounds **5a**–**5i** (MIC, nmol/mL).

Table 3. *In vitro* antibacterial and cytotoxicity activity of some potential compounds.

Table 4. Calculated molecular properties of some potential compounds.

Figure Captions

Fig. 1. Design of the quaternization harman analogues.

Fig. 2. Synthesis of compounds **3a**–**3h** and **4a**–**4x**.

Fig. 3. Synthesis of compounds **5a**–**5i**.

Fig. 4. Crystal structures of compounds **3e** and **5f**.

Fig. 5. Structure–activity relationships of the quaternization harman analogues against bacteria.

Fig. 6. SEM of MRSA and *R. solanacearum*. (A) and (C) are untreated. (B) and (D) are treated with compound **4x**.

Fig. 7. Three-dimensional conformations of compound **4x** docked in bacterial type II topoisomerase complex.

Fig. 8. Representative photographs of compound **4x** in the *in vivo* antibacterial assay: (left) untreated and (right) treated.

Table 1. *In vitro* antibacterial activities of compounds **3a**–**3h** and **4a**–**4x** (MIC, nmol/mL).[a]

Compd	Gram-positive bacteria				Gram-negative bacteria	
	S. aureus	MRSA	*B. cereus*	*B. subtilis*	*E. coli*	*R. solanacearum*
3a	>200	>200	>200	>200	>200	>200
3b	>200	>200	>200	>200	>200	>200
3c	>200	>200	>200	>200	>200	>200
3d	>200	>200	>200	>200	>200	>200
3e	>200	>200	>200	>200	>200	>200
3f	>200	>200	>200	>200	>200	>200
3g	>200	>200	>200	>200	>200	>200
3h	200	200	>200	>200	>200	>200
4a	100	200	200	100	>200	100
4b	50	50	100	50	200	50
4c	50	50	100	50	200	50
4d	100	200	200	100	>200	100
4e	50	100	50	50	>200	50
4f	25	25	25	25	200	25
4g	100	100	>200	100	>200	100
4h	50	50	100	25	100	25
4i	25	25	50	25	50	25
4j	100	100	200	50	>200	100
4k	50	50	100	25	100	25
4l	25	25	50	25	50	25
4m	>200	>200	>200	>200	>200	>200
4n	25	50	100	100	>200	50
4o	25	50	100	50	>200	50
4p	>200	>200	>200	>200	>200	>200
4q	100	100	200	100	>200	100
4r	100	100	200	100	>200	100
4s	100	100	100	50	>200	100
4t	50	50	100	25	>200	50
4u	25	25	50	25	100	25
4v	100	50	200	50	>200	50
4w	25	25	50	25	200	25
4x	25	12.5	25	25	50	25
F.S.[b]	100	50	25	12.5	6.25	50
A.S.[b]	3.125	50	200	1.56	3.125	3.125
C.S.[b]	1.56	25	25	3.125	1.56	3.125

[a]MIC = Minimum inhibitory concentration, MRSA = methicillin-resistant *S. aureus.*

[b]Positive controls, F.S. = Fosfomycin sodium, A.S. = Ampicillin sodium, C.S. = Cefotaxime sodium.

Table 2. *In vitro* antibacterial activity of compounds **5a**–**5i** (MIC, nmol/mL).

Compd	Gram-positive bacteria				Gram-negative bacteria
	S. aureus	MRSA	*B. cereus*	*B. subtilis*	*R. solanacearum*
5a	100	200	200	75	150
5b	50	100	50	50	37.5
5c	25	37.5	37.5	25	25
5d	200	200	200	100	150
5e	200	200	200	75	150
5f	75	75	100	50	50
5g	50	50	75	25	25
5h	100	>200	200	100	100
5i	100	200	200	200	100

Table 3. *In vitro* antibacterial and cytotoxicity activity of some potential compounds.

Compd	MIC (μg/mL)					Cell Viability (%)[a]	
	S. aureus	MRSA	*B. cereus*	*B. subtilis*	*R. solanacearum*	L02	MARC 145
4f	8	8	8	16	16	71.6±1.2	93.2±0.7
4i	8	8	16	8	8	76.2±1.8	87.1±1.6
4l	8	8	16	8	8	74.3±0.8	88.5±1.5
4u	8	8	16	8	8	85.7±1.4	96.3±0.9
4w	8	8	16	8	8	82.2±2.1	98.5±0.5
4x	8	4	8	16	8	84.6±1.3	103.2±2.4
5c	8	16	16	16	8	73.5±0.9	94.8±0.6
F.S.	16	8	4	2	8	-	-
A.S.	2	16	128	1	2	-	-
C.S.	1	16	16	2	2	-	-

[a]Cytotoxicity assay with potential compounds (8 μg/mL), "-" = No test.

Table 4. Calculated molecular properties of some potential compounds.

Compd	LOP[a]	TPSA[b]	nON[c]	nONNH[d]	nrotb[e]
4f	2.56	55.22	5	1	7
4i	1.50	32.82	3	1	4
4l	1.54	42.05	4	1	5
4u	2.25	38.14	4	1	4
4w	1.84	47.38	5	1	4
4x	2.28	47.38	5	1	5
5c	2.48	55.22	5	1	6

[a]LOP = octanol–water partition coefficient, [b]TPSA = topologic polar surface area, [c]nON = number of hydrogen bond acceptors, [d]nONNH= number of hydrogen bond donors, [e]nrotb = number of rotatable bonds.

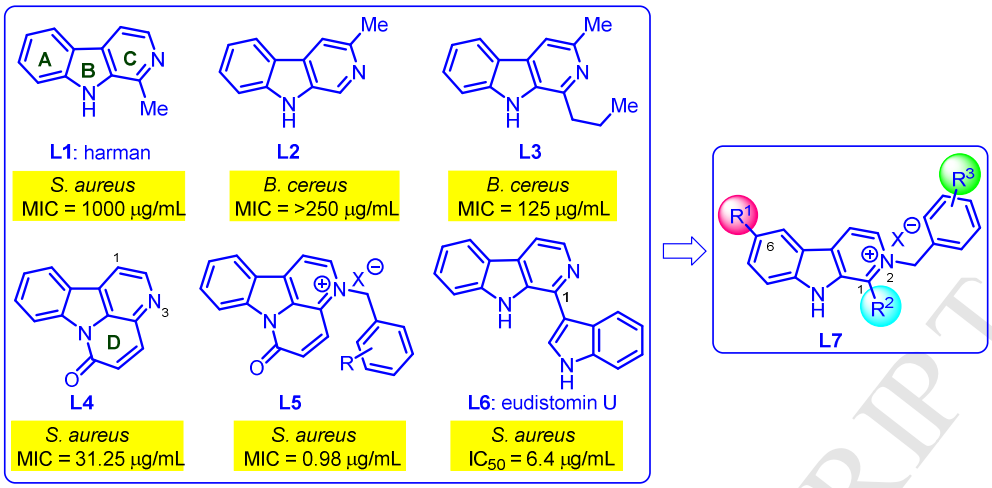

Fig. 1. Design of the quaternization harman analogues.

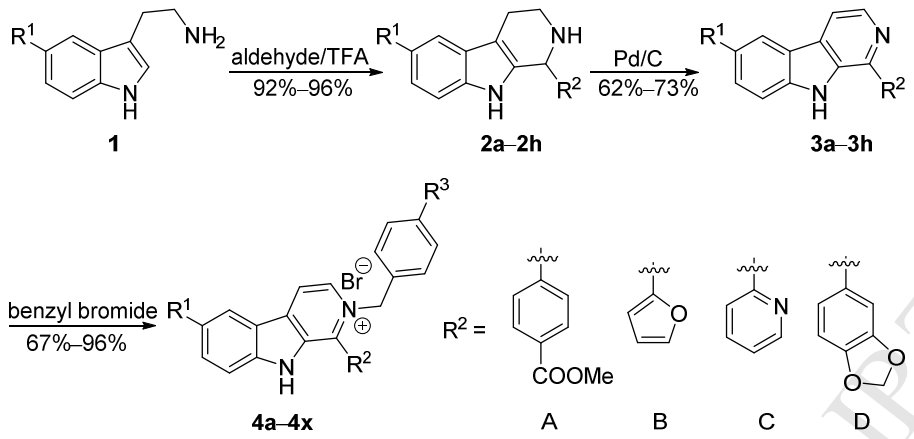

	R^1	R^2		R^1	R^2	R^3		R^1	R^2	R^3		R^1	R^2	R^3
3a	H	A	**4a**	H	A	H	**4i**	H	B	CF_3	**4q**	OMe	C	Me
3b	OMe	A	**4b**	H	A	Me	**4j**	OMe	B	H	**4r**	OMe	C	CF_3
3c	H	B	**4c**	H	A	CF_3	**4k**	OMe	B	Me	**4s**	H	D	H
3d	OMe	B	**4d**	OMe	A	H	**4l**	OMe	B	CF_3	**4t**	H	D	Me
3e	H	C	**4e**	OMe	A	Me	**4m**	H	C	H	**4u**	H	D	CF_3
3f	OMe	C	**4f**	OMe	A	CF_3	**4n**	H	C	Me	**4v**	OMe	D	H
3g	H	D	**4g**	H	B	H	**4o**	H	C	CF_3	**4w**	OMe	D	Me
3h	OMe	D	**4h**	H	B	Me	**4p**	OMe	C	H	**4x**	OMe	D	CF_3

Fig. 2. Synthesis of compounds **3a**–**3h** and **4a**–**4x**.

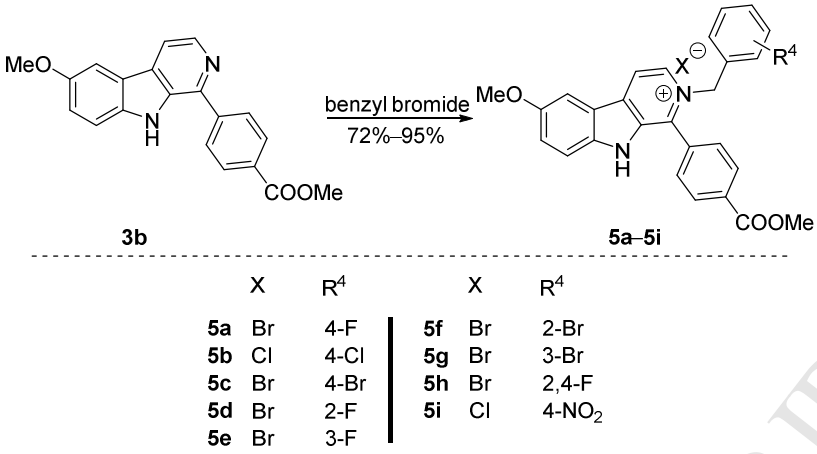

3b **5a–5i**

	X	R^4		X	R^4
5a	Br	4-F	**5f**	Br	2-Br
5b	Cl	4-Cl	**5g**	Br	3-Br
5c	Br	4-Br	**5h**	Br	2,4-F
5d	Br	2-F	**5i**	Cl	4-NO_2
5e	Br	3-F			

Fig. 3. Synthesis of compounds **5a**–**5i**.

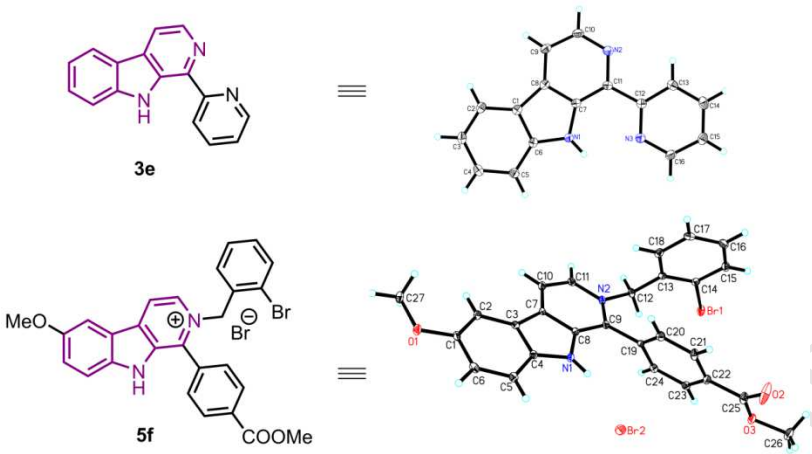

Fig. 4. Crystal structures of compounds **3e** and **5f**.

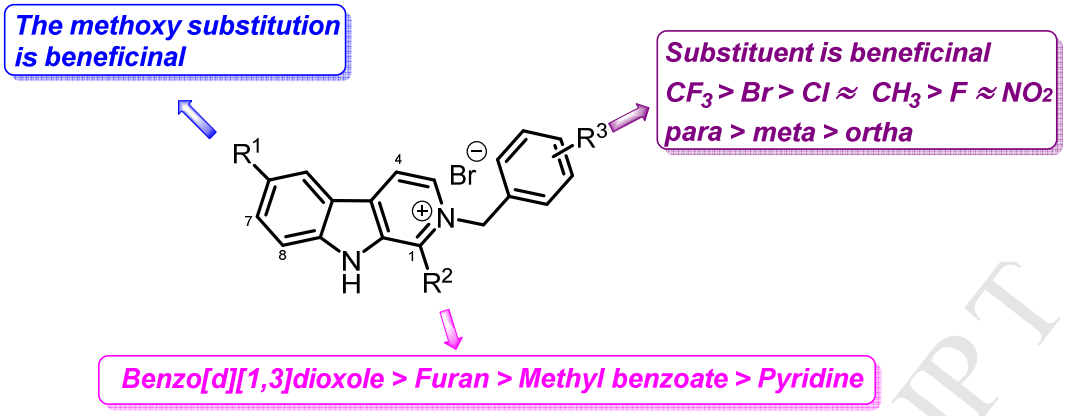

Fig. 5. Structure–activity relationships of the quaternization harman analogues against bacteria.

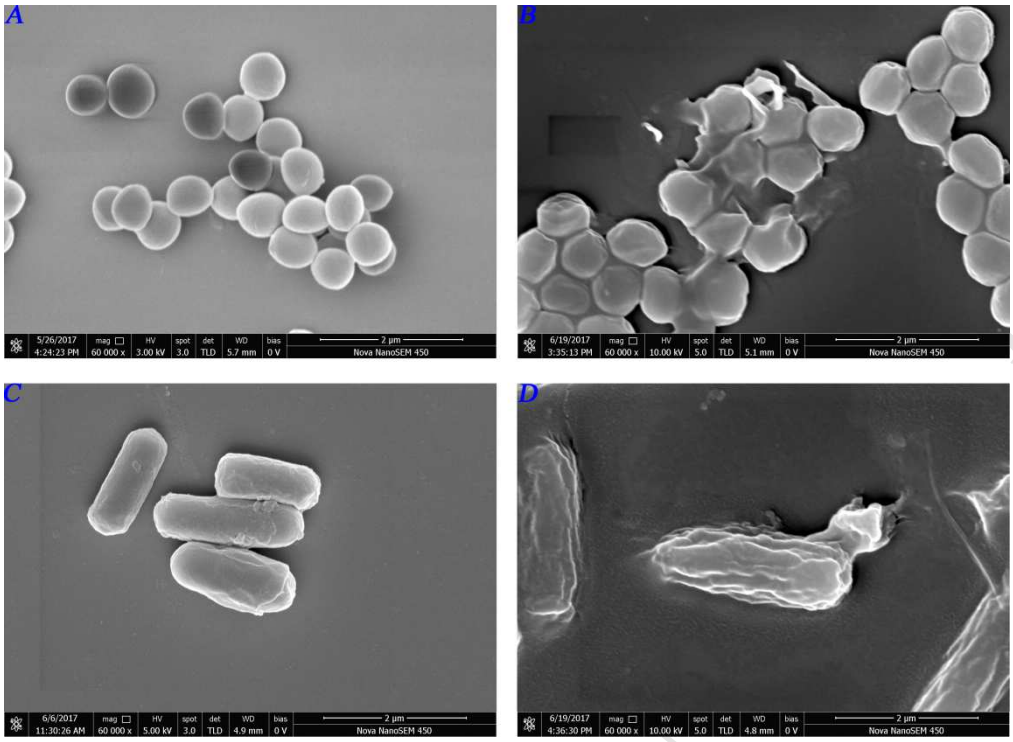

Fig. 6. SEM of MRSA and *R. solanacearum*. (A) and (C) are untreated. (B) and (D) are treated with compound **4x**.

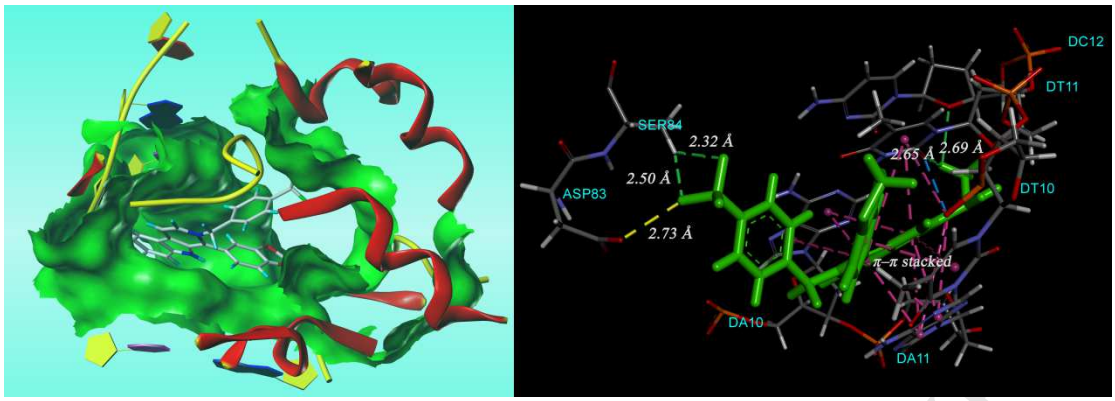

Fig. 7. Three-dimensional conformations of compound **4x** docked in bacterial type II topoisomerase complex.

Fig. 8. Representative photographs of compound **4x** in the *in vivo* antibacterial assay: (left) untreated and (right) treated.

Highlights

- Thirty-three new quaternization harman analogues were synthesized and the peak MIC was 4 μg/mL.
- The structure–activity relationships were summarized.
- The compound **4x** showed low cytotoxicity, good thermal stability and "drug-like" properties.
- The compound **4x** could damage the bacterial cell membrane and wall, and disrupt the function of type II topoisomerase.